

Article

Optimizing Microgrid Performance: Integrating Unscented Transformation and Enhanced Cheetah Optimization for Renewable Energy Management

Ali S. Alghamdi 

Department of Electrical Engineering, College of Engineering, Majmaah University, Majmaah 11952, Saudi Arabia; aalghamdi@mu.edu.sa

Abstract: The increased integration of renewable energy sources (RESs), such as photovoltaic and wind turbine systems, in microgrids poses significant challenges due to fluctuating weather conditions and load demands. To address these challenges, this study introduces an innovative approach that combines Unscented Transformation (UT) with the Enhanced Cheetah Optimization Algorithm (ECO) for optimal microgrid management. UT, a robust statistical technique, models nonlinear uncertainties effectively by leveraging sigma points, facilitating accurate decision-making despite variable renewable generation and load conditions. The ECO, inspired by the adaptive hunting behaviors of cheetahs, is enhanced with stochastic leaps, adaptive chase mechanisms, and cooperative strategies to prevent premature convergence, enabling improved exploration and optimization for unbalanced three-phase distribution networks. This integrated UT-ECO approach enables simultaneous optimization of continuous and discrete decision variables in the microgrid, efficiently handling uncertainty within RESs and load demands. Results demonstrate that the proposed model significantly improves microgrid performance, achieving a 10% reduction in voltage deviation, a 10.63% decrease in power losses, and an 83.32% reduction in operational costs, especially when demand response (DR) is implemented. These findings validate the model's efficacy in enhancing microgrid reliability and efficiency, positioning it as a viable solution for optimized performance under uncertain renewable inputs.

Keywords: microgrid management; renewable energy integration; operational efficiency improvement; unscented transformation; uncertainty propagation; enhanced cheetah optimization algorithm



Citation: Alghamdi, A.S. Optimizing Microgrid Performance: Integrating Unscented Transformation and Enhanced Cheetah Optimization for Renewable Energy Management.

Electronics **2024**, *13*, 4563. <https://doi.org/10.3390/electronics13224563>

Academic Editors: Temitayo Olowu and Raghav Khanna

Received: 29 September 2024

Revised: 8 November 2024

Accepted: 11 November 2024

Published: 20 November 2024



Copyright: © 2024 by the author. Licensee MDPI, Basel, Switzerland. This article is an open access article distributed under the terms and conditions of the Creative Commons Attribution (CC BY) license (<https://creativecommons.org/licenses/by/4.0/>).

1. Introduction

The increasing integration of renewable energy sources (RESs), particularly photovoltaic (PV) systems and wind turbines (WTs), is transforming the power sector, though it also introduces significant challenges due to their inherent variability. These sources, while clean, are intermittent and heavily influenced by weather conditions, which complicates the management of microgrids (MGs) and necessitates robust optimization approaches. Solar and wind energy availability fluctuates based on factors such as sunlight exposure and wind speed, while additional uncertainties stem from varying consumer loads, demand response (DR) programs, and electric vehicle (EV) charging behaviors [1–4]. The need to handle these uncertainties has led to advanced optimization techniques, with hybrid algorithms demonstrating promise in terms of enhancing MG operations. For instance, a combined PSO and Bat Algorithm (BAPSO) has been applied to optimize solar PV configurations in microgrids, effectively reducing transmission losses and enhancing efficiency [5]. Other approaches integrate various storage and backup systems, employing hybrid algorithms such as zebra optimization and artificial gorilla troops optimizers for maximum power point tracking, achieving substantial improvements in resource utilization and response times [6]. Likewise, demand-side management strategies incorporating hybrid techniques like SHO-MDACGAN have shown potential in minimizing operating costs and

improving power stability in PV-based microgrids [7]. Additionally, a novel Gravitational Particle Swarm Optimization Algorithm (GPSOA) that combines the strengths of PSO and the gravitational search algorithm (GSA) has proven effective in addressing combined economic and emission dispatch (CEED) challenges in wind–thermal systems by balancing fuel costs and emission reduction objectives [8]. Another sequential hybrid algorithm, the PSO-GSA (HPSO-GSA), with dependent random coefficients has demonstrated enhanced exploration abilities, making it a robust approach for complex optimization scenarios where premature stagnation is a concern [9].

To address the operational uncertainty, accurate modeling techniques such as Monte Carlo Simulation (MCS) and the Point Estimate Method (PEM) are frequently used [10,11]. Integrating these uncertainty quantification methods with hybrid optimization algorithms can effectively optimize both operational costs and reliability in MGs, enhancing energy management while balancing efficiency and adaptability [12]. Among the widely used techniques for handling uncertainty in renewable energy sources and load demand is MCS. The technique involves the simulation of different scenarios generated from probability distributions of input variables like solar radiation, wind speed, and load profiles. Accurate results are indeed obtained with MCS, although with very high computational complexity, especially in large systems. For instance, Ahn et al. have used the sequential MCS method for scenario estimations, which involves electric, cooling, and heating demand combined with solar irradiance [13]. Other works have also discussed the effectiveness of MCS in regard to scenario generation and energy management in MGs [4,14,15].

In contrast, the PEM provides a computationally efficient alternative by approximating the statistical behavior of random variables using specific points. In fact, the PEM has been applied to several energy management systems of MGs when computation time with desired accuracy is of interest. Alavi et al. in [16] utilized the PEM for modeling power exchanges and optimizing the operations of MGs within uncertain conditions. Further studies [17,18] emphasize the potential of the application of the PEM to enhance performance while reducing computational burdens in various microgrid approaches. According to [19], the PEM cannot handle correlated variables and its error can increase with the standard deviation of a random input variable.

UT is a nonlinear analytical method that propagates the mean and covariance of input variables through a nonlinear function [20]. It relies on a reduced number of deterministically calculated samples (sigma points) that capture the statistical distribution of uncertain variables. The UT is simple to apply and requires low computational time to estimate the mean and covariance of desired variables [19]. In [21], a comparison of the UT method, MCS and the PEM is presented in detail. The previous works have presented the application of the UT method to solve the probabilistic power flow issues in an unbalanced three-phase microgrid [22], a balanced islanded microgrid with renewable sources [20], and to provide a power flow solution for a transmission and distribution system [23].

These uncertainties could be dispersed only by using advanced optimization techniques. The optimization methods available in the literature for microgrid energy management problems may be broadly classified into two groups: classical techniques and metaheuristics optimization algorithms. Classical techniques mainly comprise mixed-integer linear programming (MILP) and mixed-integer quadratic programming (MIQP), which are quite useful in modeling the on/off states of generators and loads [24]. Yet, most of them require some form of linearization in order to be able to handle the complexity; hence, there is the development of mixed-integer quadratically constrained programming (MIQCP), although, in many optimization scenarios, this may not be suitable [25].

Traditional methods include linear programming, quadratic programming, and MILP, which provide accuracy but are not capable of handling dynamic variables such as market prices and weather variability with ease [26–28]. The applications of gradient descent, Quasi-Newton, and Powell's method fall short because most are stuck to a local optimum point [29–31].

Compared to the limitations mentioned above, metaheuristic and heuristic algorithms can further allow for flexibility and efficiency in terms of handling complex nonlinear problems. Algorithms of particular note are genetic algorithms (GAs) [32], particle swarm optimization (PSO) [33], and evolutionary optimization techniques. Indeed, as an example of this potential, one hybrid evolutionary optimization algorithm was utilized with stochastic multi-objective optimization in microgrids within an approach where wind power forecasts were integrated to lessen the computational load and reduce time consumption [34]. GAs, indeed, have proven to be useful in applications, as they are able to slice optimization by time up to 23% [35].

Metaheuristic algorithms are exceptionally good at dealing with the intrinsic complexity of microgrid energy management. By their very nature, these algorithms are bio-inspired and do not make any assumptions about the problem being solved. They make use of probabilistic search, local investigation, and global optimization techniques. The technique known as PSO has been used to optimize microgrid performance by solving complex optimization problems regarding control and fault detection [36–38]. Ant colony optimization (ACO) has also been applied to energy management with the intent of minimizing operational costs and enhancing renewable energy utilization [39]. Other highlighted MHOAs are the salp swarm optimization algorithm (SSA) [40], GAs [41], the whales optimization algorithm (WOA) [42], and gray wolf optimization (GWO) [43], since each will come forth with varied benefits in regard to tackling microgrid optimization challenges.

They ensure convergence to the optimum solution; however, due to the generally non-convex problems in microgrid energy management, traditional methods of mathematical programming cannot handle them [44]. The metaheuristic algorithms discussed above could be a flexible and computationally efficient alternative solutions for possibly dealing with nonlinearities–uncertainties possessed by microgrid systems. Hence, such approaches are currently desired for MGs because of their simplicity and ability towards reducing computational efforts.

Despite the emergence of various approaches to modeling uncertainties and optimization techniques in microgrids, most of the gaps still remain. MCS is able to model renewable energy sources and load demands accurately with high precision but also introduces high computational complexity, especially for large-scale systems. On the contrary, the PEM offers computational efficiency but limits handling correlated variables and increases error when higher standard deviations are experienced. Traditional methods in optimization, like MILP and quadratic programming, are based on linearization techniques that may not fit well with the complex nature of microgrid problems. On the other hand, a number of promises from metaheuristic algorithms like the GA and PSO can solve complex optimization issues. However, notwithstanding their promising potential, most of these conventional methods inherently suffer from a number of drawbacks, such as premature convergence, nonlinearities handling difficulty, and balancing exploration and exploitation processes. These result in mediocre near-global optima, especially for complex systems like microgrids with renewable energy sources that have a high variability and uncertainty. While both of these methods assure reasonable global search capabilities, solution fine-tuning in the latter stages of optimization is relatively poor, which leads to reduced system performance for adaptability and precision-intensive scenarios.

The original conventional cheetah optimization (CO) [45], inspired by the hunting behavior of cheetahs, overcame several challenges by increasing the balance between exploration and exploitation. However, like many other conventional algorithms, it still suffers from a number of limitations regarding global exploration, especially while dealing with complex multi-objective problems involving high uncertainty. In application to unbalanced three-phase distribution networks, appropriate optimization of both continuous and discrete decision variables might not be achieved by the CO due to its tendency towards premature convergence in view of fluctuating renewable energy and load demands. Advanced methods are thus of utmost necessity in handling their inherent uncertainties and improving, in general, the operational efficiency of microgrids. Combining these

methods with advanced uncertainty modeling approaches for unbalanced three-phase distributions is still a challenge. In fact, there is a real need for better methods that are capable of integrating all the strengths of uncertainty modeling and different optimization techniques in order to enhance efficiency and reliability in microgrids.

This work integrates UT and the ECOA for optimal microgrid planning and operation. The system under investigation is an imbalanced three-phase distribution system and therefore bridges the highlighted research gaps. This paper extends earlier research by:

- Applying UT to model uncertainty propagation in nonlinear functions for the more accurate transmission of uncertainty in terms of renewable energy supply and load demand. This technique avoids a couple of major limitations associated with MCS and the PEM in the imbalanced three-phase distribution system, given the lower computational workload involved in modeling the uncertainties.
- The advanced metaheuristic optimization algorithm inspired by cheetahs' hunting nature proposes stochastic leaps and adaptive chase mechanism cooperation approaches that enhance the global exploration capability by removing it from premature convergence in order to converge into a robust solution for complicated optimization problems in unbalanced three-phase systems.
- UT and ECOA inclusions create a comprehensive framework within our approach to continuous and discrete optimization variables of microgrid operations. A combination of UT will improve resilience in managing uncertainties in renewable energy sources and load demand for efficient unbalanced three-phase distribution systems.
- The proposed framework can reduce network losses by 10.63%, operational costs by 83.32%, and voltage profile variation by 10% when simulation results are considered. In addition, the inclusions of DR programs further enhance the efficiency of the system and the highly effective and dependable paradigm for microgrid planning and operation in unbalanced three-phase distribution networks.
- The paper contributes by applying and comparing the performances of the GA, PSO, conventional CO, and two hybrid algorithms, such as GPSOA and HPSO-GSA, in the optimal management of microgrids. It further indicates the weaknesses of both the GA and PSO in dealing with uncertainties and falling into the local optima. The CO drains more, though it still shows its weakness in highly complex scenarios. These comparisons highlight the importance of the ECOA, which is able to yield better results in terms of minimizing power losses, voltage deviation, and overall cost of operation.

In a nutshell, this research further develops the state of the art in terms of microgrid optimization through a methodology that overcomes the main limitations affecting existing approaches to the problem thanks to advanced uncertainty modeling combined with sophisticated optimization techniques, conceived for unbalanced three-phase distribution systems.

The paper is organized as follows: Section 2 elaborates on problem formulation, including a description of the objectives and constraints of the microgrid optimization problem. Section 3 describes Unscented Transformation in uncertainty modeling while examining the use of UT in dealing with the intermittency of renewable energy sources. Section 4 elaborates on the proposed algorithm, investigating the integration of UT into the ECOA. Section 5 gives the simulation results, showing the performance comparison between the proposed method and conventional approaches. Conclusions are drawn in Section 6, which also summarizes the main findings and proposes future research directions.

2. Problem Formulation

The objective of the research is to find, out of several generation options, the most efficient energy management approach in a three-phase unbalanced MG. This means the minimization of operational critical metrics (i.e., the total cost, including costs caused by emission, operation, and maintenance) and assurance of voltage stability with a minimum

of active power losses. In this regard, the problem is a multi-objective optimization problem subjected to microgrid operational and stability requirements.

2.1. Decision Variables

The problem includes the nature of the optimization procedure involved in a microgrid operation that possesses a mix of characteristics, including continuous and discrete decision variables. These are subsequently categorized below:

The continuous variables can be defined for this problem as the power outputs and the flows at every time-step t :

- $P_{PV}(t)$: Active power output from the PV system.
- $P_{WT}(t)$: Active power output from the WT.
- $P_{DR}(t)$: Power reduction achieved through DR.
- $P_{Grid}(t)$: Power purchased from the main grid.
- $P_{BESS}(t)$: Power associated with charging or discharging the battery energy storage system (BESS).
- $P_{DG}(t)$: Active power generated by the diesel generator (DG).
- $P_{MT}(t)$: Active power generated by the microturbine (MT).

These variables are collectively expressed as:

$$X_{\text{cont}} = [P_{PV}(t), P_{WT}(t), P_{DR}(t), P_{Grid}(t), P_{BESS}(t), P_{DG}(t), P_{MT}(t)] \quad \forall t \in \mathcal{T} \quad (1)$$

The discrete decision variables determine the bus and phase allocations for distributed energy resources (DERs), which are crucial for managing three-phase imbalances in the microgrid.

- Bus Allocation Variables (B_{bus}):

$$B_{\text{bus}} = [B_{PV}(t, b), B_{WT}(t, b), B_{DR}(t, b), B_{Grid}(t, b), B_{BESS}(t, b), B_{DG}(t, b), B_{MT}(t, b)] \quad \forall b \in \mathcal{B}, \forall t \in \mathcal{T} \quad (2)$$

where $B_{\text{DER}}(t, b)$ indicates the bus location b for each DER at time t .

- Phase Assignment Variables (B_{phase}):

$$B_{\text{phase}} = [\phi_{PV}(t, p), \phi_{WT}(t, p), \phi_{DR}(t, p), \phi_{Grid}(t, p), \phi_{BESS}(t, p), \phi_{DG}(t, p), \phi_{MT}(t, p)] \quad \forall p \in \mathcal{P}, \forall t \in \mathcal{T} \quad (3)$$

where $\phi_{\text{DER}}(t, p)$ denotes the phase p (A, B, or C) assigned to each DER at time t .

The full set of decision variables for the optimization problem is:

$$X = [X_{\text{cont}}, X_{\text{disc}}] \quad \forall t \in \mathcal{T} \quad (4)$$

2.2. Objective Functions

The optimization problem is formulated to minimize the following three objective functions:

2.2.1. Total Power Losses (J_1)

$$J_1 = \sum_{l=1}^{L_{\text{lines}}} (r_l^a \cdot I_l^a(t)^2 + r_l^b \cdot I_l^b(t)^2 + r_l^c \cdot I_l^c(t)^2) \quad \forall t \in \mathcal{T} \quad (5)$$

where r_l^a , r_l^b , and r_l^c are the resistances of line l in phases A, B, and C, respectively, and $I_l^a(t)$, $I_l^b(t)$, and $I_l^c(t)$ are the corresponding line currents.

2.2.2. Voltage Deviation (J_2)

This objective ensures voltage levels across all buses and phases remain within acceptable limits.

$$J_2 = \frac{1}{3} \times (\sqrt{\sum_{n=1}^{N_{\text{bus}}} (1 - |V_n^a(t)|)^2} + \sqrt{\sum_{n=1}^{N_{\text{bus}}} (1 - |V_n^b(t)|)^2} + \sqrt{\sum_{n=1}^{N_{\text{bus}}} (1 - |V_n^c(t)|)^2}) \quad (6)$$

2.2.3. Total Cost (J_3)

$$J_3 = C_{PV}(t) + C_{WT}(t) + C_{BESS}(t) + C_{DG}(t) + C_{MT}(t) + C_{Grid}(t) + C_{DR}(t) \quad (7)$$

- Cost of PV and WT Systems.

The total cost of PV and WT systems can be expressed as:

$$C_{RES,\zeta}(t) = C_{FIX,\zeta} + C_{VAR,\zeta} \times P_{\zeta}(t) \quad \forall t \in \mathcal{T}, \forall \zeta \in \{PV, WT\} \quad (8)$$

In this equation, $C_{RES,\zeta}(t)$ is the total cost of the renewable energy source ζ (which could be a PV system or WT) at time t . The term $C_{FIX,\zeta}$ represents the fixed cost, $C_{VAR,\zeta}$ is the variable cost of the renewable energy source ζ , while $P_{\zeta}(t)$ is the power output of source ζ at time t .

The fixed cost is calculated as:

$$C_{FIX,\zeta} = \frac{C_{INV,\zeta} \times r}{(1 - (1 + r)^{-T_{Life}}) \times 8760 \times CF_{\zeta}} \quad (9)$$

Here, $C_{INV,\zeta}$ represents the initial investment cost of source ζ , r is the discount rate, T_{Life} is the expected lifetime of the system in years, and CF_{ζ} is the capacity factor of source ζ . The number 8760 represents the total hours in a year.

The variable cost is given by:

$$C_{VAR,\zeta} = C_{O\&M,\zeta} \quad (10)$$

In this case, $C_{O\&M,\zeta}$ is the operation and maintenance cost for the renewable energy source ζ .

- Cost of the BESS

The cost of the BESS (battery energy storage system) operation is expressed as:

$$C_{BESS}(t) = C_{FIX,BESS} + (C_{CHG} \times P_{BESS}^{ch}(t) + C_{DSG} \times P_{BESS}^{ds}(t)) + \gamma_{TOU}(t) \times P_{BESS}(t) \quad (11)$$

This equation then gives the overall cost of operating the BESS at time t . Note that $C_{BESS}(t)$ is the total cost of the BESS operation at time t , $C_{FIX,BESS}$ is the fixed cost of the BESS, and the terms C_{CHG} and C_{DSG} then represent the variable charging and discharging costs, respectively, while $P_{BESS}^{ch}(t)$ and $P_{BESS}^{ds}(t)$ are the power charged to and discharged from the BESS at time t . $\gamma_{TOU}(t)$ is the time-of-use (TOU) electricity price at time t ; $P_{BESS}(t)$ is the total BESS power (both charging and discharging) at time t .

The fixed cost of the BESS is calculated as:

$$C_{FIX,BESS} = \frac{C_{INV,BESS} \times r}{(1 - (1 + r)^{-T_{Life,BESS}}) \times 8760 \times CF_{BESS}} \quad (12)$$

Here, $C_{INV,BESS}$ is the investment cost of the BESS, r is the discount rate, $T_{Life,BESS}$ is the expected lifetime of the BESS in years, and CF_{BESS} is the capacity factor of the BESS. The number 8760 represents the total hours in a year.

The variable costs of charging and discharging are expressed as:

$$C_{CHG} = C_{O\&M,CHG}, \quad C_{DSG} = C_{O\&M,DSG} \quad (13)$$

where $C_{O\&M,CHG}$ and $C_{O\&M,DSG}$ are the operation and maintenance costs for charging and discharging the BESS, respectively.

- Cost of DG, MT, and Grid Power

The cost of operating DG, MT, and grid power systems is modeled as:

$$C_{GEN,\zeta}(t) = C_{FUEL,\zeta}(t) + C_{EMI,\zeta}(t) + C_{O\&M,\zeta}(t) \quad \forall t \in \mathcal{T}, \forall \zeta \in \{DG, MT, Grid\} \quad (14)$$

where

$$C_{\text{FUEL},\xi}(t) = \alpha_{\xi} \times P_{\xi}(t) + \beta_{\xi} \times P_{\xi}^2(t) + \gamma_{\xi} \tag{15}$$

$$C_{\text{EMI},\xi}(t) = (\mu_{\text{CO}_2} + \mu_{\text{SO}_2} + \mu_{\text{NO}_x}) \times P_{\xi}(t) \tag{16}$$

$$C_{\text{O\&M},\xi}(t) = \kappa_{\xi} \times P_{\xi}(t) \tag{17}$$

Specific equations are as follows, in which $C_{\text{GEN},\xi}(t)$ is the total generation cost of technology ξ , at time t , which includes fuel cost $C_{\text{FUEL},\xi}(t)$, emission cost $C_{\text{EMI},\xi}(t)$, and operation and maintenance cost $C_{\text{O\&M},\xi}(t)$, while $P_{\xi}(t)$ is the power output of technology ξ at time t . The form of the fuel cost function contains a linear term with coefficient α_{ξ} and a quadratic term with coefficient β_{ξ} . The emission cost depends on the unit costs for the emissions of CO_2 , SO_2 , and NO_x , labeled by μ_{CO_2} , μ_{SO_2} , and μ_{NO_x} , respectively. Operation and maintenance costs depend on coefficient κ_{ξ} . ξ is in use for different generation technologies, such as DG, MT, and the grid, while \mathcal{T} represents the set of time periods under consideration.

Finally, $C_{\text{DR}}(t)$ represents the costs associated with DR at time t :

$$C_{\text{DR}}(t) = \beta_{\text{I/C}} \times P_{\text{DR}}(t) + \lambda \times \mathbb{E}[\text{VSI}(t)] \tag{18}$$

In this equation, $\beta_{\text{I/C}}$ represents the cost coefficient for interruptible or curtailable loads, while $P_{\text{DR}}(t)$ denotes the voluntary load reduction at time t . The parameter λ serves as a weighting factor for balancing cost and grid stability, and $\mathbb{E}[\text{VSI}(t)]$ stands for the expected voltage stability.

For unifying the scales of these objectives, each objective function is normalized:

$$J'_i = \frac{J_i - J_i^{\min}}{J_i^{\max} - J_i^{\min}} \quad \forall i \in \{1, 2, 3\} \tag{19}$$

The aggregate objective function to be minimized is:

$$J_{\text{total}} = J'_1 + J'_2 + J'_3 \tag{20}$$

2.3. Dynamic Pricing-Based DR

This DR program encourages a load reduction in response to real-time electricity prices. The reduction in power due to DR is modeled as:

$$P_{\text{DR}}(t) = \gamma \times \left(\frac{\pi(t)}{\pi_{\text{base}}} \right) \times \sum_{i=1}^N P_{\text{Load}}(t, i) \tag{21}$$

where $P_{\text{DR}}(t)$ is the power reduction at time t due to DR, γ is a proportionality constant reflecting the sensitivity of the load to price changes, $\pi(t)$ is the real-time electricity price at time t , and π_{base} is the base-line price. $\sum_{i=1}^N P_{\text{Load}}(t, i)$ represents the total load, which is the sum of the individual consumer loads at time t , where N reflects the total number of consumers.

This formulation would be subject to the following constraints:

$$-\alpha(t) \times \sum_{i=1}^N P_{\text{Load}}(t, i) \leq P_{\text{DR}}(t) \leq \alpha(t) \times \sum_{i=1}^N P_{\text{Load}}(t, i) \tag{22}$$

where $\alpha(t)$ is the utmost allowable load reduction or increase, ensuring that the DR does not exceed certain limits.

2.4. Adaptive Load Shedding Algorithm

The adaptive load shedding algorithm dynamically optimizes load reduction to minimize total operational costs while maintaining grid stability:

$$\min_{P_{\text{DR}}(t)} (C_{\text{total}}(t) + \lambda \times \mathbb{E}[\text{VSI}(t)]) \tag{23}$$

In this equation, $C_{\text{total}}(t)$ represents the total operational cost at time t , λ is a weighting factor that balances the cost and grid stability, and $\mathbb{E}[\text{VSI}(t)]$ is the expected value of the voltage stability index (VSI) at time t , which measures the grid's stability under the current load conditions.

2.5. Constraints

The optimization is subject to several constraints, ensuring the microgrid operates within its physical and operational limits:

2.5.1. Power Flow Constraints

- Active Power Balance:

$$P_{\text{PV}}(t) + P_{\text{WT}}(t) + P_{\text{DG}}(t) + P_{\text{MT}}(t) + P_{\text{Grid}}(t) + P_{\text{DR}}(t) \pm P_{\text{BESS}}(t) = P_{\text{Load}}(t) + P_{\text{loss}}(t) \quad (24)$$

This equation ensures that the total power supply equals the demand plus losses at all times. Here, $P_{\text{PV}}(t)$ is the power generated by the PV system at time t , $P_{\text{WT}}(t)$ is the WT power output, $P_{\text{DG}}(t)$ is the power from DG, and $P_{\text{MT}}(t)$ is the power from MT. The power imported from the main grid is denoted by $P_{\text{Grid}}(t)$, while the power reduction resulting from DR is denoted by $P_{\text{DR}}(t)$. The power of the BESS is denoted by the term $P_{\text{BESS}}(t)$, which can be either positive (discharging) or negative (charging). $P_{\text{Load}}(t)$ represents the entire load demand on the demand side, while $P_{\text{loss}}(t)$ represents the power losses in the system.

- Reactive Power Flow:

$$Q_{\text{flow}}(n, t, m, p) = \sum_{m \in \mathcal{B}} (|V_n(t, p)| \cdot |V_m(t, p)| \cdot |Y_{nm}| \cdot \sin(\theta_n(t, p) - \theta_m(t, p) - \phi_{nm}(t, p))) \quad (25)$$

This equation represents the reactive power flow between nodes in the power system. Here, $Q_{\text{flow}}(n, t, m, p)$ denotes the reactive power flowing from node n to node m at time t with phase p . The term $|V_n(t, p)|$ is the magnitude of the voltage at node n and $|V_m(t, p)|$ is the magnitude of the voltage at node m . $|Y_{nm}|$ represents the magnitude of the admittance between nodes n and m . The angle difference $\theta_n(t, p) - \theta_m(t, p)$ is adjusted by the phase angle $\phi_{nm}(t, p)$, which accounts for the phase shift introduced by the admittance. The sine function captures the reactive power component of the flow.

2.5.2. Voltage and Current Limits

- Line Current Limits:

$$|I_l(t, p)| \leq I_{l, \text{max}} \quad \forall l \in L_{\text{lines}}, \forall t \in \mathcal{T}, \forall p \in \mathcal{P} \quad (26)$$

This constraint ensures that the current flowing through each transmission line l does not exceed its maximum allowable value $I_{l, \text{max}}$ at any time t and for any phase p .

- Voltage Magnitude Limits:

$$V_{\text{min}} \leq |V_n(t, p)| \leq V_{\text{max}} \quad \forall n \in \mathcal{B}, \forall t \in \mathcal{T}, \forall p \in \mathcal{P} \quad (27)$$

This constraint ensures that the voltage magnitude at each node n remains within the specified minimum V_{min} and maximum V_{max} limits at all times t and under all conditions p .

2.5.3. DER Operational Limits

$$0 \leq P_{\zeta}(t) \leq P_{\zeta, \text{max}} \quad \forall \zeta \in \{\text{PV}, \text{WT}, \text{BESS}, \text{DG}, \text{MT}, \text{Grid}\}, \forall t \in \mathcal{T} \quad (28)$$

This constraint ensures that the power output $P_{\zeta}(t)$ from each type of distributed energy resource (DER) ζ is within the range from 0 to its maximum allowable output $P_{\zeta, \text{max}}$ at all times t .

2.5.4. Integer Constraints

$$1 \leq B_{bus}, B_{phase} \leq N_{bus}, N_{phase} \tag{29}$$

This constraint ensures that the integer variables B_{bus} and B_{phase} are within the allowable range, where N_{bus} and N_{phase} represent the total number of buses and phases, respectively.

3. UT for Uncertainty Modeling

In modern microgrids, the integration of renewable energy sources, like PV systems and WTs, introduces considerable uncertainty in terms of their operation due to the variability of weather conditions. Consequently, there is intrinsic uncertainty in load demand, which makes energy management even more complicated [34]. We employ UT as a robust way of propagating uncertainty through nonlinear functions describing the operation of the microgrid.

UT is a statistical methodology that is used to calculate the mean and covariance of a random variable that undergoes a nonlinear transformation. Unlike traditional methods, such as MCS, UT relies on a deterministic sampling technique, called sigma points, to accurately capture the mean and variance of the transformed variable using minimal computational resources [19,46].

In the context of the modeling of the microgrid, the most important uncertainties are considered to be produced by a case of renewable energy generation and one of load demand. The generation of renewable energy, such as from PV systems and WTs, varies due to changes in irradiance and wind speed, respectively. Similarly, load demand follows a temporal pattern that changes with the time of day, climatic and meteorological conditions, as well as with consumers' patterns of behavior.

3.1. UT Procedure

Let \mathbf{Z} be the vector of uncertain variables comprising renewable generation and load demand. UT is applied to propagate this uncertainty through nonlinear power flow equations as well as the overall optimization problem.

For an n -dimensional random variable, \mathbf{Z} with mean, $\bar{\mathbf{Z}}$ and a covariance matrix, \mathbf{P}_Z UT determines $2n + 1$ sigma points $\{\mathbf{Z}_i\}_{i=0}^{2n}$ according to the following formulae:

$$\mathbf{Z}_0 = \bar{\mathbf{Z}} \tag{30}$$

$$\mathbf{Z}_i = \bar{\mathbf{Z}} + \left(\sqrt{(n + \lambda)\mathbf{P}_Z} \right)_i, \quad i = 1, 2, \dots, n \tag{31}$$

$$\mathbf{Z}_{i+n} = \bar{\mathbf{Z}} - \left(\sqrt{(n + \lambda)\mathbf{P}_Z} \right)_i, \quad i = 1, 2, \dots, n \tag{32}$$

where λ is a scaling parameter given by $\lambda = \alpha^2(n + \kappa) - n$, where α is a small positive constant and κ is a secondary scaling parameter.

Each of the sigma points, \mathbf{Z}_i , is propagated through the nonlinear functions modeling the power flow equations and operational constraints of the microgrid. For a nonlinear function $\mathbf{f}(\cdot)$, the transformed sigma points are computed as:

$$\mathbf{Y}_i = \mathbf{f}(\mathbf{Z}_i), \quad i = 0, 1, \dots, 2n \tag{33}$$

The mean and covariance of the transformed variable \mathbf{Y} are estimated as:

$$\bar{\mathbf{Y}} = \sum_{i=0}^{2n} W_i^{(m)} \mathbf{Y}_i \tag{34}$$

$$\mathbf{P}_Y = \sum_{i=0}^{2n} W_i^{(c)} (\mathbf{Y}_i - \bar{\mathbf{Y}})(\mathbf{Y}_i - \bar{\mathbf{Y}})^T \tag{35}$$

where $W_i^{(m)}$ and $W_i^{(c)}$ are weights for the mean and covariance, respectively:

$$W_0^{(m)} = \frac{\lambda}{n + \lambda}, \quad W_0^{(c)} = \frac{\lambda}{n + \lambda} + (1 - \alpha^2 + \beta) \quad (36)$$

$$W_i^{(m)} = W_i^{(c)} = \frac{1}{2(n + \lambda)}, \quad i = 1, \dots, 2n \quad (37)$$

Here, β is a parameter that incorporates prior knowledge of the distribution of \mathbf{Z} , such as $\beta = 2$ for Gaussian distributions.

3.2. Incorporating UT into Microgrid Optimization

This is where, in the microgrid optimization problem, the UT algorithm enhances the problem capability for handling uncertainties involved in renewable generation and load demand. The incorporation of UT will hence make the optimization framework capable of handling the mentioned uncertainty in the objective functions and constraints effectively. This can be written as considering the robustness in the final solution against the inherent variability in the system for UT-generated sigma points in the objective functions, which include total cost, voltage deviation, and power losses.

Putting this into a modified objective function, including the uncertainty provided by the following:

$$J_{\text{total}}^{\text{UT}} = \sum_{i=0}^{2n} W_i^{(m)} J_{\text{total}}(\mathbf{X}, \mathbf{Z}_i) \quad (38)$$

where $J_{\text{total}}(\mathbf{X}, \mathbf{Z}_i)$ is the total objective function evaluated at the i -th sigma point \mathbf{Z}_i and \mathbf{X} is the vector of decision variables.

Furthermore, the constraints are checked at all the sigma points to ensure that the constraints are valid along the range of the uncertain variables. This may be expressed as:

$$\text{Subject to : } g_k(\mathbf{X}, \mathbf{Z}_i) \leq 0, \forall k, \forall i = 0, 1, \dots, 2n \quad (39)$$

This concept keeps the microgrid's operational states within safe limits of operations, given the uncertainties in renewable energy generation and load demand. The incorporation of UT into the optimization problem gives robustness to the problem for the more reliable and efficient operation of microgrids.

4. The Proposed Algorithm

4.1. Overview of the Cheetah Optimizer (CO)

The CO is an optimization algorithm inspired by the hunting strategy of cheetahs [45]. It is based on the different strategies that a cheetah deploys in locating its prey, such as scanning, stalking, and rapid acceleration, that enable it to efficiently locate and capture the hunted object. The CO could demonstrate promising performance in regard to various optimization problems due to its appropriate balance between exploration and exploitation through different intelligent search strategies. However, while the CO is good at finding near-optimal solutions, there are some issues in terms of evading the local optima and keeping diversity in the search space. These might engender premature convergence and poor performance in complex high-dimensional optimization problems.

We try to address these challenges by proposing the Enhanced Cheetah Optimization Algorithm, which tries to improve upon the original CO by introducing dynamic and adaptive mechanisms that amplify global exploration and finesse in the exploitation phase. The ECOA avoids such risk from the local optima, further increasing the convergence speed and enhancing the overall robustness of the algorithm in solving such complex optimization tasks using introduced stochastic processes and cooperative strategies.

4.2. Enhanced Cheetah Optimization Algorithm (ECOA)

The ECOA is an enhanced version of the original Cheetah Optimizer. In the enhanced variant of the Cheetah Optimization Algorithm, the mechanism of exploration and exploitation has become much more sophisticated, involving several major adaptive mechanisms and stochastic processes that enhance performance and avoid the local optima. Below, the key elements of the ECOA are outlined.

4.2.1. Exploration by Stochastic Jump Strategy

The ECOA's exploration is based on a stochastic jump technique inspired by Lévy flights. This method allows for big, dynamic jumps in the search space, which contributes to improved global exploration. During iteration $t + 1$, the position of the i -th cheetah in the j -th dimension is updated:

$$X_{i,j}^{(t+1)} = X_{\text{leader},j}^t + \epsilon \cdot \text{Lévy}(j) \cdot \gamma_{i,j}^t \quad (40)$$

where

- $X_{\text{leader},j}^t$ is the leader position in the j -th dimension at iteration t .
- ϵ is a small positive constant controlling the jump intensity.
- $\text{Lévy}(j)$ is a random vector derived from the Lévy distribution.
- $\gamma_{i,j}^t$ is the step size at iteration t , dynamically adjusted based on the cheetahs' relative position.

The step size of $\gamma_{i,j}^t$ in Equation (40) changes dynamically in the ECOA, using the cheetah's role and position in the population, i.e., it naturally balances the exploration and utilization through this adaptive mechanism:

$$\gamma_{i,j}^t = \kappa \cdot (X_{\text{prey},j}^t - X_{i,j}^t), \quad (41)$$

where κ is a scaling factor that depends on the amount of distance that one is from optimum.

The second-best solution guides the search in Equation (40). In every iteration, $X_{\text{leader},j}^t$ drives the search. In such a way, the ECOA refines the search in regions around the best-known solutions, improving convergence:

4.2.2. Stationary Ambush Strategy

If the ECOA finds promising regions, then a stationary ambush strategy is employed which saves energy by reducing all unnecessary movements. Early convergence is prevented, with the position update rule being defined as:

$$X_{i,j}^{(t+1)} = X_{i,j}^t \quad (42)$$

This would imply that the cheetah does not move from its position to maintain stability.

4.2.3. Adaptive Chase Mechanism

The ECOA introduces an adaptive chase mechanism during the exploitation phase, wherein cheetahs adjust their positions based on the optimal solution (prey). The position update is defined as:

$$X_{i,j}^{(t+1)} = X_{\text{prey},j}^t + \eta_{i,j} \cdot \zeta_{i,j}^t \quad (43)$$

where $\eta_{i,j}$ is the randomness factor, simulating unpredictable movements during the chase. $\zeta_{i,j}^t$ represents the cooperative interaction factor.

The ECOA enhances the performance by incorporating a mechanism of cooperative interaction among cheetahs. This mechanism helps to increase cooperation inside the population, significantly enhancing convergence rates and robustness against local optima:

$$\zeta_{i,j}^t = X_{i,j}^t - X_{k,j}^t \quad (44)$$

Here, $X_{k,j}^t$ is upper neighborhoods (other cheetah position at the same dimension developing the cooperative search).

The psedue-code of ECOA is summarized in Table 1.

Table 1. Pseudo-code for the ECOA.

Step	Description	Equation/Details
1	Define parameters	D : dimensionality, n : population size, MaxIt: maximum iterations
2	Generate initial population	Generate X_i^0 for $i = 1, 2, \dots, n$ and evaluate fitness
3	Initialize iteration counter	$t \leftarrow 1$
4	Main loop	While $t \leq \text{MaxIt}$ do
5	Sort and select	Sort population, select prey X_{prey} and leader X_{leader}
6	Iterate over each cheetah	For each cheetah i do
7	Select neighbor	Select neighbor cheetah k
8	Randomly select dimensions	$\mathcal{J} \subset \{1, 2, \dots, D\}$, size $d = \left\lceil \frac{D}{\text{rand}_i \left\lceil \frac{D}{3} \right\rceil} \right\rceil$
9	Stationary ambush	$X_{i,j}^t \leftarrow X_{i,j}^{(t-1)}$ for all $j \in \mathcal{J}$
10	Calculate parameters	Update H_i^t
11	Ambush condition	If $H_i^t > 0.25$ then
12	Exploration strategy	$X_{i,j}^{(t+1)} \leftarrow X_{\text{Prey},j}^t + \epsilon \cdot \text{Lévy}(j) \cdot \gamma_{i,j}^t$
13	Otherwise, use exploitation	Else
14	Exploitation strategy	$X_{i,j}^{(t+1)} = X_{\text{prey},j}^t + \eta_{i,j} \cdot \zeta_{i,j}^t$
15	End condition check	End If
16	Update position	Update $X_{i,j}^{(t+1)}$ if new position is better
17	End cheetah iteration	End For
18	Update best solutions	Update prey X_{prey} and leader X_{leader}
19	Increment iteration	$t \leftarrow t + 1$
20	End main loop	End While
21	Return best solution	Return X_{prey} as the best solution

The ECOA achieves automatic optimal parameter acquisition through several adaptive strategies that dynamically adjust as the algorithm progresses. First, the stochastic jump strategy enhances global exploration by using Lévy flights to allow for large, adaptive jumps in the search space. The step size $\gamma_{(i,j)}^t$ adjusts automatically based on each cheetah’s position and role, facilitating a smooth transition from exploration in early stages to exploitation as optimal solutions are approached.

In the adaptive chase mechanism, cheetahs modulate their positions relative to the optimal (prey) solution, using both a randomness factor $\eta_{(i,j)}$ and a cooperative interaction factor $\zeta_{(i,j)}^t$. This dual adjustment creates an inherent balance between the exploration and exploitation phases without the need for manual tuning, as it adapts in real-time to the search landscape.

Finally, cooperative interaction among cheetahs contributes to efficient convergence by fostering collaboration between individuals in the population, helping to prevent premature convergence to local optima. This adaptive cooperation among neighboring solutions automatically tunes parameters to enhance both convergence speed and robustness. Together, these strategies enable the ECOA to perform optimally across complex, unbalanced three-phase distribution networks, facilitating both global and local searches without manual parameter settings.

4.3. Implementation of the Proposed Methodology

The steps for solving the problems involved in operation and planning in microgrids using the ECOA and UT for handling uncertainties are shown in Figure 1 and briefly explained as follows:

- Step 1: Define input data.
 - Initialization of the microgrid data includes the prices for the electric energy, the load data, and the characteristics of the DERs.
 - All the parameters of the algorithm have to be determined: the size of the population, the number of iterations, and the parameters of UT, i.e., the number of uncertain variables and their respective probability density functions.
- Step 2: Reduce the problem to an unrestricted form.

Convert the constrained optimization problem into an unconstrained one, penalizing all constraint violations by using a penalty function so that all the solutions satisfy the operational and safety limits of the microgrid.
- Step 3: Generation of initial population.

Generate an initial population of solutions for the ECOA. Each solution is a feasible microgrid operation configuration that are generated within prescribed limits; in cases when constraint violations occur, the solutions are repaired to make them feasible.
- Step 4: Evaluate the objective function using UT.

For each population solution, use UT to propagate the uncertainty in renewable energy generation and load demand through the power flow equations. Determine the sigma points for each parameter that is unknown. Transform the sigma points using the nonlinear microgrid functions and then calculate the goal function $2n + 1$ times, where n represents the number of unknown parameters. Calculate the expected value of the objective function based on the results of UT.
- Step 5: Choose the best solution.

Keep the best solution, which has the lowest predicted cost or objective value among the analyzed population.
- Step 6: Apply the ECOA Improvisation Stage.

Update the population using ECOA improvisation mechanisms; explore and exploit the solution space through interactions between the prey, leader, and other cheetahs.
- Step 7: Improvements to the CO.

Improve the quality of the solutions and increase the convergence and variety of the population by applying the ECOA's specific variation operators to the newly updated population.
- Step 8: Conclusion.

The algorithm terminates if any of the termination criteria (the utmost number of iterations or the stated objective function value) are satisfied. If they are not, proceed to Step 4 to continue refining and iterating the solutions.

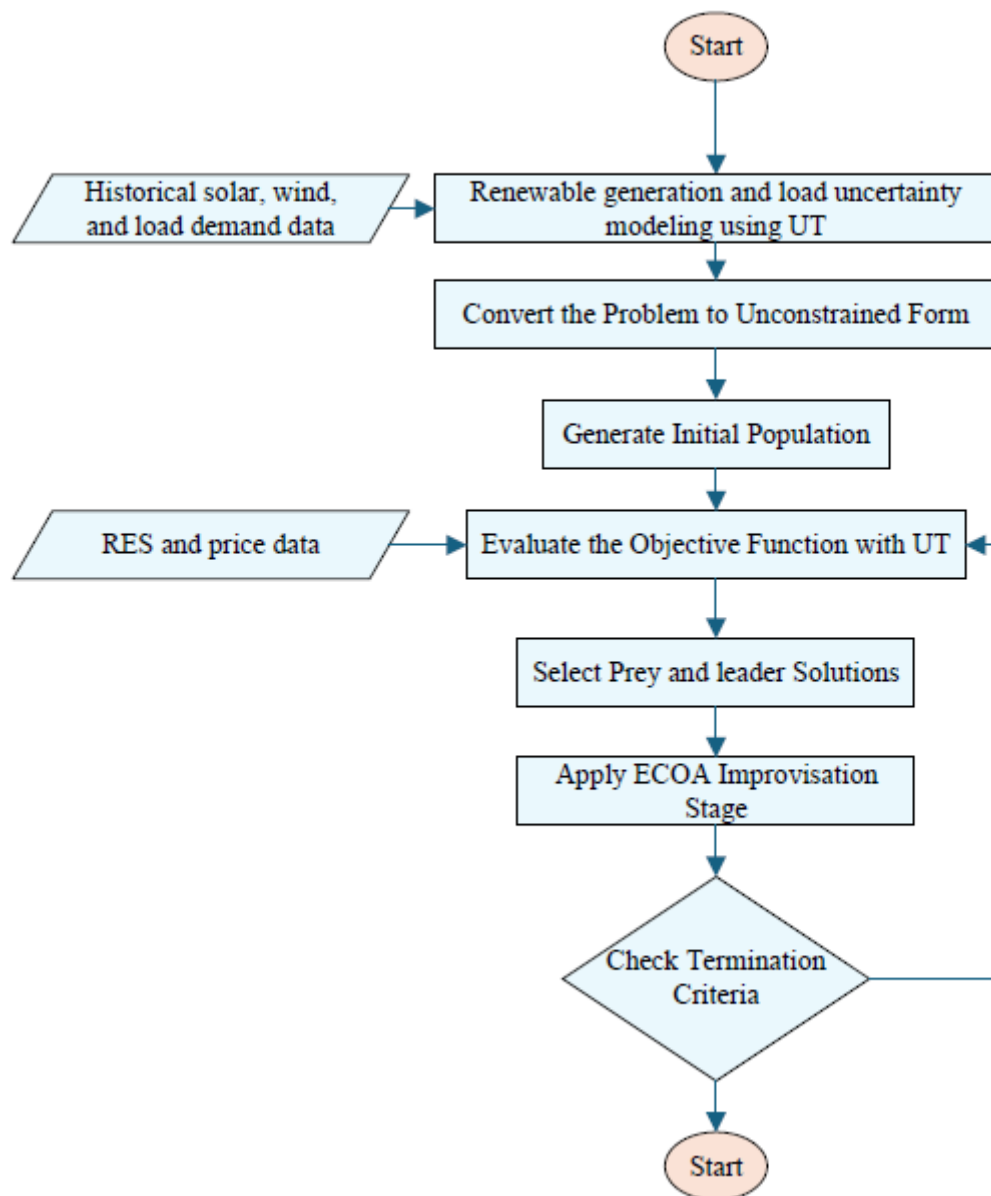


Figure 1. Flowchart of the proposed UT-based ECOA for optimal solving of EM problems.

5. Simulation Results

5.1. Overview of the Simulated Microgrid System

The difficulties of integrating large amounts of RESs, including PV systems and WTs, into an imbalanced three-phase distribution network are handled by the simulated microgrid system. The model records the dynamic interactions between changing renewable energy and changing load needs using the IEEE 13-bus test system [47]. Essential technical details of the generation units can be found in Table 2 [48–50]. In addition, the hourly active power production of the WT and PV and the hourly load demand forecast are shown in Figure 2. Based on current laws, particularly those set by the Ontario energy board, the model's DR behavior should be affected by its use of a TOU pricing system. In this scenario, grid electricity accounts for 50% of the base load, MTs provide 10%, and the remaining demand is met by PV systems, WTs, and the BESS. Stochastic weather patterns and fluctuating demand are used to simulate the real-time fluctuation of RES output and load situations. The methodology will find the best power-generating mix—PV systems, WTs, DGs, MTs, and the BESS—by integrating DR programs and striking a balance between

supply and demand. The optimization was performed using the ECOA in conjunction with UT for uncertainty management.

Table 2. Parameters of the utilized resources in the model.

Generation Source	Parameter (Unit) Value					
MT	μ_{CO_2} (kg/kWh)	μ_{SO_2} (kg/kWh)	μ_{NO_x} (kg/kWh)	β_{ζ} (USD/kWh)	α_{ζ} (USD/kWh)	γ_{ζ} (USD/h)
	0.72	0.002	0.091	0.000018	0.03872	1.356
DG	μ_{CO_2} (kg/kWh)	μ_{SO_2} (kg/kWh)	μ_{NO_x} (kg/kWh)	β_{ζ} (USD/kWh)	α_{ζ} (USD/kWh)	γ_{ζ} (USD/h)
	0.65	0.093	4.483	0.0002	0.03632	1.65
PV	$C_{INV,\zeta}$ (USD)	$C_{O\&M,\zeta}$ (USD/kW)	CF_{ζ}	T_{Life} (years)		
	6675×400	0.012	0.3	25		
WT	$C_{INV,\zeta}$ (USD)	Oper.cost (USD/kW)	CF	T_{Life} (years)		
	1500×400	0.00952	0.2	20		
BESS	$C_{INV,BESS}$ (USD)	$C_{O\&M,CHG} / C_{O\&M,DSG}$ (USD/kW)	CF_{BESS}	$T_{Life,BESS}$ (years)		
	1775×200	0.05	0.25	25		
Grid	μ_{CO_2} (kg/kWh)	μ_{SO_2} (kg/kWh)	μ_{NO_x} (kg/kWh)			
	0.85	2.14	9.723			
DR	$\beta_{I/C}$ (USD/kWh)					
	0.1					

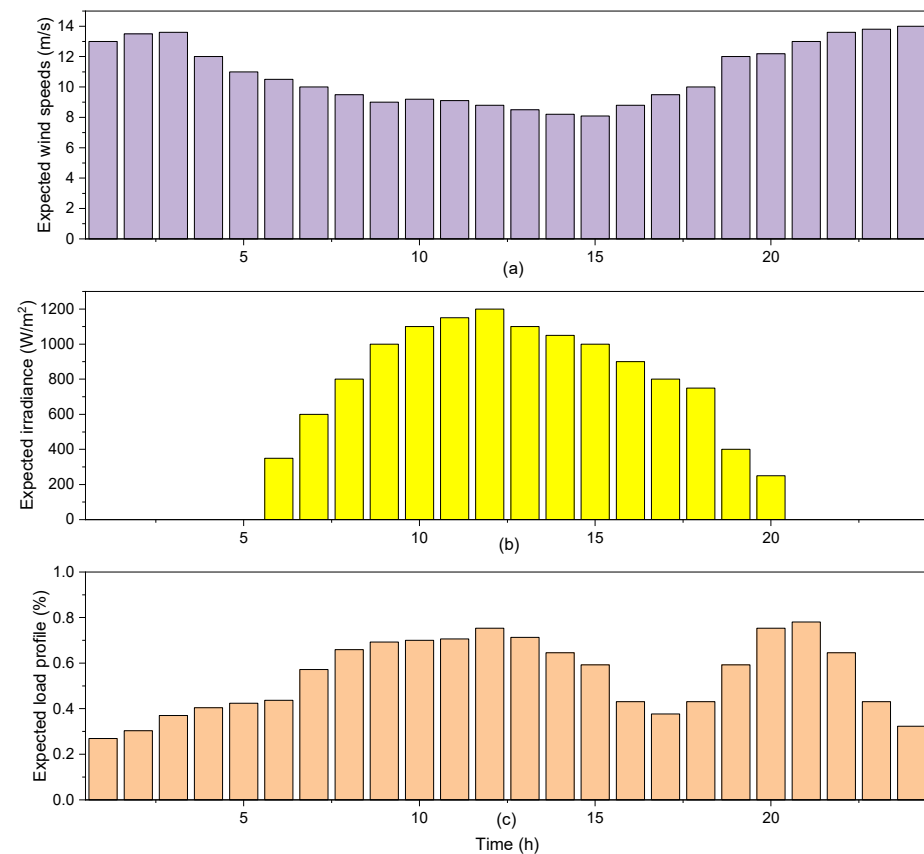


Figure 2. The mean values of (a) wind speed, (b) solar irradiance, and (c) load demand.

The simulation parameters are chosen to ensure that the results are robust: 25 runs with 100 iterations and a population size of 50 for each procedure. The conventional CO, PSO, and GA, as well as two hybrid algorithms (GPSOA and HPSO-GSA), were compared, and testing revealed that the ECOA performed better in terms of cost minimization and energy supply optimization under uncertainty. All simulations were run in MATLAB R2021b on a PC with an Intel i5 processor, 4 GB RAM, and a CPU speed of 2.5 GHz. This can assure steady performance in computationally intensive optimization processes. The established approach can provide practical and scalable insights into how a microgrid operates, allowing for a full assessment of system efficiency and dependability.

5.2. Optimal Power Generation and Resource Contribution (Continue Variables)

The proposed methodology is used to find the optimal power generation performances inside a microgrid provided with distributed sources like PV systems, WTs, DGs, MTs, and the BESS. It also implements various DR programs. The proposed model captures the temporal variability of the power output of these sources to simulate the performance under variant conditions, as depicted in Figure 3.

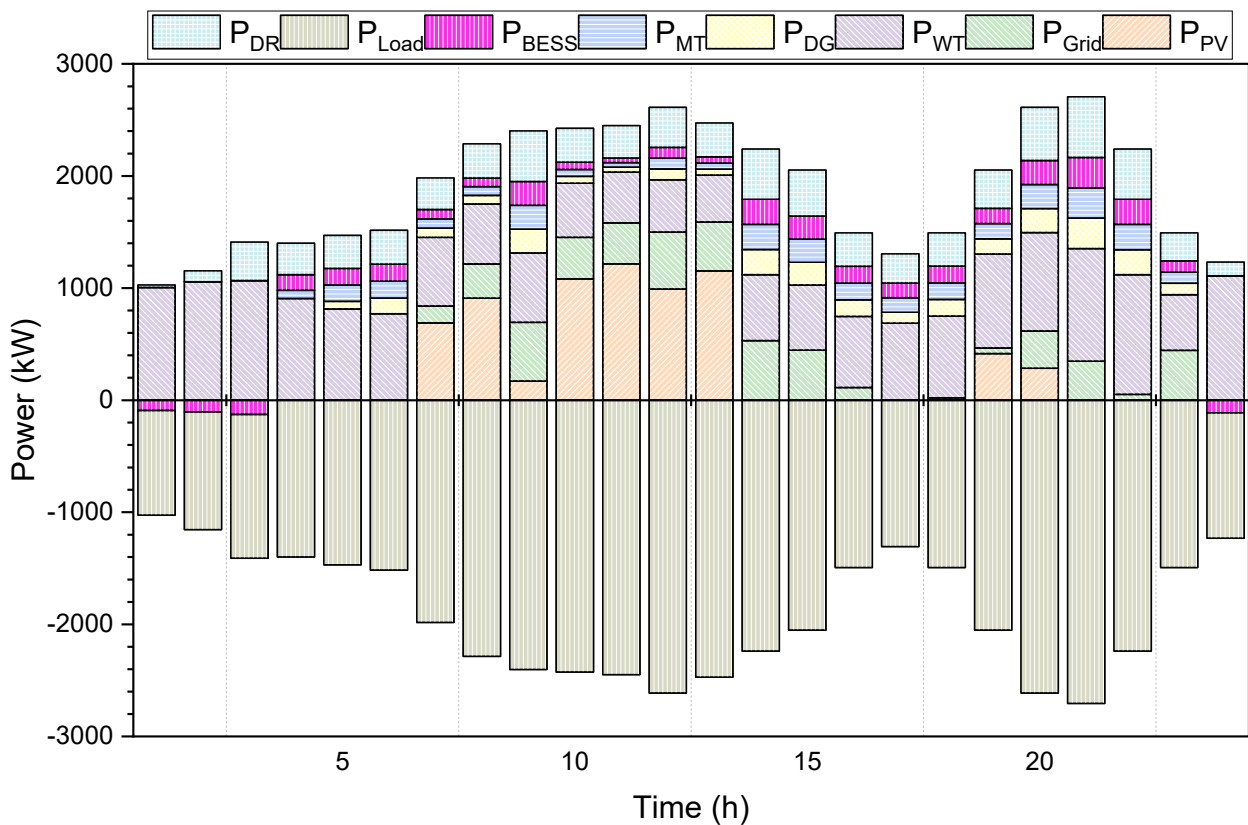


Figure 3. Microgrid's Optimal generation scheduling.

The generated PV generation is very negligible in most of the night-time hours (for example, from hour 1 to hour 5). However, from hour 6, it increases further to midday, reaching a maximum output of 991.2684 kW at hour #12. The WTs produce a decent amount relatively stably throughout the day; their peak generation is at hour 19, which is 837.6866 kW, showing that wind energy is one of the most reliable renewable resources inside the microgrid. Utility grid power usage varies by the availability of the local generation. In this case, during low output of the renewable energy sources (from hour 1 to 5 h), utility grid power contributes a minimum, peaking at hour 14 with 531.3536 kW, where demand and the amount drawn from the microgrid are higher. Dispatchable sources such as DGs and MTs are of paramount importance for backup power, especially during periods when the generation from renewable sources is at an all-time low. The peak output for diesel

generators falls at hour 9, with 211.9006 kW, while peak output for microturbines falls at hour 5, with 146.9435 kW, contributing quite effectively during these high-demand periods.

The BESS has a significant role that involves smoothing the microgrid energy fluctuations, absorbing the surplus power during low demand, and releasing the stored energy at peak demand. From this perspective, negative values in the BESS output signify charging states, while positive values denote discharging states. For instance, a BESS charged during hours 1–5, when renewable generation is limited, gains extra energy by absorbing the negative values of -93.24 kW, -104.79 kW, and -128.02 kW to enhance its storage capacity. On the other hand, this extra stored energy is utilized efficiently during peak demand periods to meet the high demand while easing the dependence on the grid, as in hour 10, where the BESS discharges 62.78 kW. This interaction between the BESS and other sources, such as WT and PV systems, provides an optimum balance between energy supply and demand during the day, thus improving the general efficiency and reliability of the microgrid.

In fact, DR programs have proven to be efficient in reshaping the load curve, especially during peak demand hours. The modified load, after the application of DR, is shown in Figure 4 and indicates a critical reduction in demand from hours 7 to 21. For example, the original load of hour 9 was 1949.73 kW, which throttles down to 1242.08 kW after the application of DR. This provided a smoothening effect on the load profile and will reduce the strain that would otherwise have been placed on the generation units, thus adding to the system efficiency.

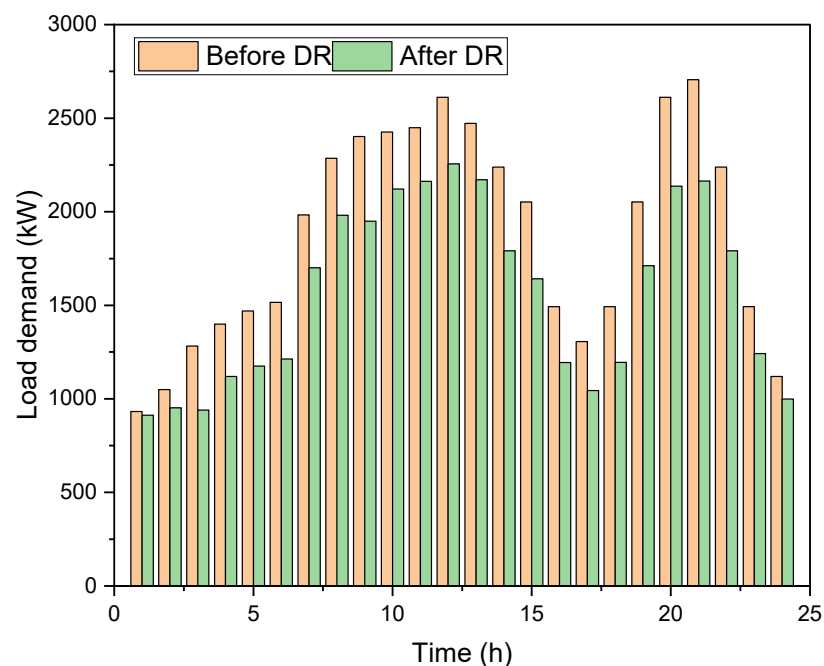


Figure 4. DR's effect on the hourly load curve.

5.3. Impact of TOU Pricing on Microgrid Operations

TOU pricing, therefore, grants influence over the optimization of microgrid operations through segmenting electricity costs into three distinct periods: off-peak at 8.7 ¢/kWh, mid-peak at 12.2 ¢/kWh, and on-peak at 18.2 ¢/kWh. This form of pricing encourages the shifting of power generation and consumption for both economic efficiency and operational reliability.

- Off-Peak Period (Hours 1–6 and 20–24)

From Figure 3, when the off-peak hour is considered to have the lowest price of electricity, the microgrid prioritizes charging the BESS. The negative values of the BESS in those periods show the state of the BESS while charging, absorbing excess generation. Still, at hour 1, -93.24 kW is utilized from the BESS due to the optimization of energy costs.

The wind generation also starts to kick in, albeit at a lower level; therefore, WTs can supply base energy. This will pretty effectively minimize reliance on the more expensive grid electricity as the ESS builds its charge for later use.

- Mid-Peak Period: 7–10 h; 17–19 h

During the mid-peak hours of the TOU pricing, WTs and the BESS begin to become more important in terms of maintaining generation and load balance (see Figure 3). A WT will start giving its contribution fully with an approximate 630.3 kW output during such mid-peak periods to help reduce reliance on expensive grid electricity. Meanwhile, the BESS moves into a discharge state, providing power to reduce further costs. For instance, in hour 8, it supplies 76.22 kW, which shows that it utilizes the stored energy efficiently to meet the demand in the period of high pricing.

- On-Peak Period [Hours 11–16]

It is at this point that the microgrid operates when the electricity prices are highest; it concentrates its strategy on maximizing the deployment of local renewable energy sources, such as PV systems. As such, during hour 10, for example, the output of PV reaches its peak of 1083.23 kW and thus reduces dependence on highly expensive grid power. The WT still provides a considerable amount of energy, with the output reaching 452.73 kW at hour 11; hence, it is important for the minimization of the operational costs because of peak pricing. Combining these sources will enable the microgrid system to function during periods of high demand without incurring many utility costs.

DR programs also emerge as one of the most essential strategies in all periods. For instance, as shown in Figure 4, at hour 12, DR reduces the load from 2255.29 kW to 1127.64 kW and, hence, works effectively while shifting consumption at a time when the prices are high. Throughout the process, as shown, the cumulative effect of DR enhances the microgrid to match the consumption based on the pricing structure. This saves stress on the grid and also encourages economic efficiency. The efficient TOU pricing methodology, the optimal generation of WTs, charging and discharging of the energy storage system, and DR programs together effectively enhance the operational efficiency of the microgrid. An overall cost reduction in operational costs amounting to 80% from scenarios without such optimization measures is a testament to the success of this integrated approach in fostering economic viability while ensuring a reliable and sustainable energy supply.

5.4. Optimal Location-Specific Performance Analysis (Discrete Variables)

The analysis of the optimal generation results points to the performance of not only each generation option but also specific locations and phases that are important from the point of view of the distribution network. In that respect, efficiency in the delivery of power can be guaranteed together with system reliability at different load conditions during the course of the day.

According to the results indicated in Figure 5, regarding PV generation, the optimal performance is in Bus 2, Phase A, where solar energy generation is at its peak in the afternoon. This area receives ideal sunlight, which makes it a perfect site to mount a PV system. Other phases have relatively smaller outputs of PV, especially Bus 1 and Bus 4, which further illustrates the need for proper site selection to tap into the full potential of solar resources effectively.

Figure 6 also identifies Bus 2 as one of the highly contributing buses across all phases, especially in Phase A and Phase B, which can contribute significant robustness to utility supply in the stabilization process during periods of smaller renewable outputs.

Figure 7 shows the results of the dispersed WT generation; it can be seen that the highest contributions are obtained at Bus 2 in Phase A, particularly during the early hours of the morning. This sort of pattern characterizes the good wind conditions of this point; it means that wind installations must consider the geographical aspect of siting. The other buses, like Bus 1 and Bus 4, show low wind output; hence, siting becomes an important aspect to be considered in regard to WTs.

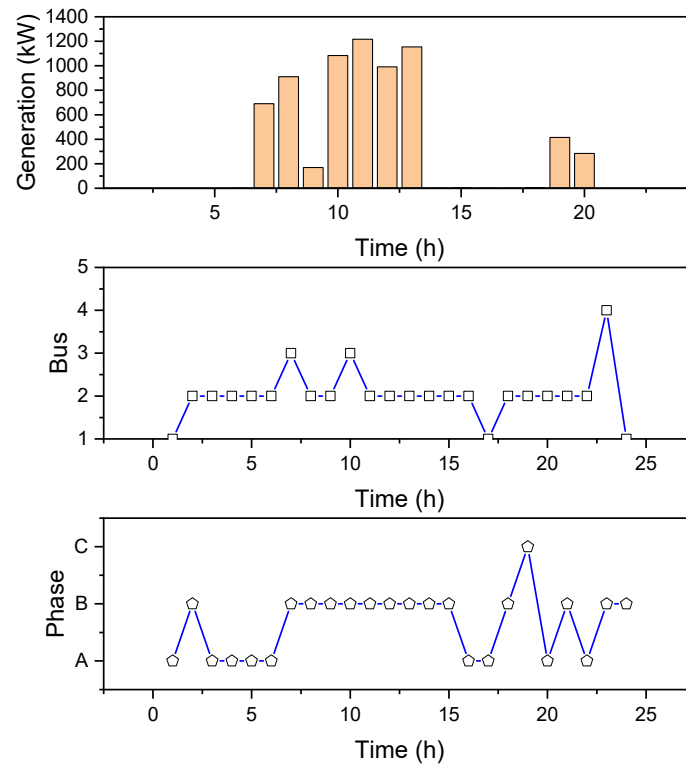


Figure 5. Optimal results of the PV's power generation, bus, and phase locations.

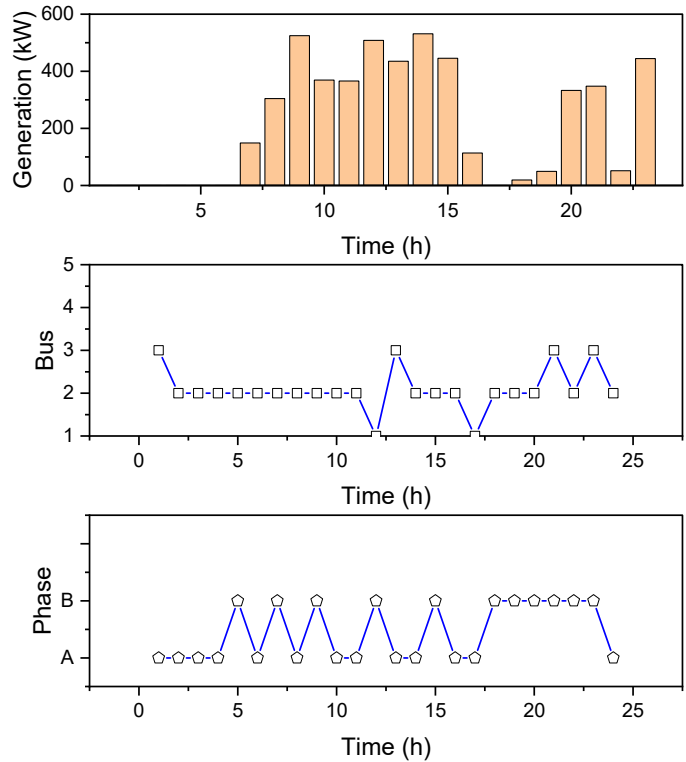


Figure 6. Optimal results of the grid's power generation, bus, and phase locations.

Figure 8 further presents the DG at Bus 2, Phase A, which features continued optimal output, resonating with its capability of delivering steady power throughout the day. The installations of DGs within the subject phase are appropriately positioned to support fluctuating renewable generation and hence deliver a steady supply during peak demand periods.

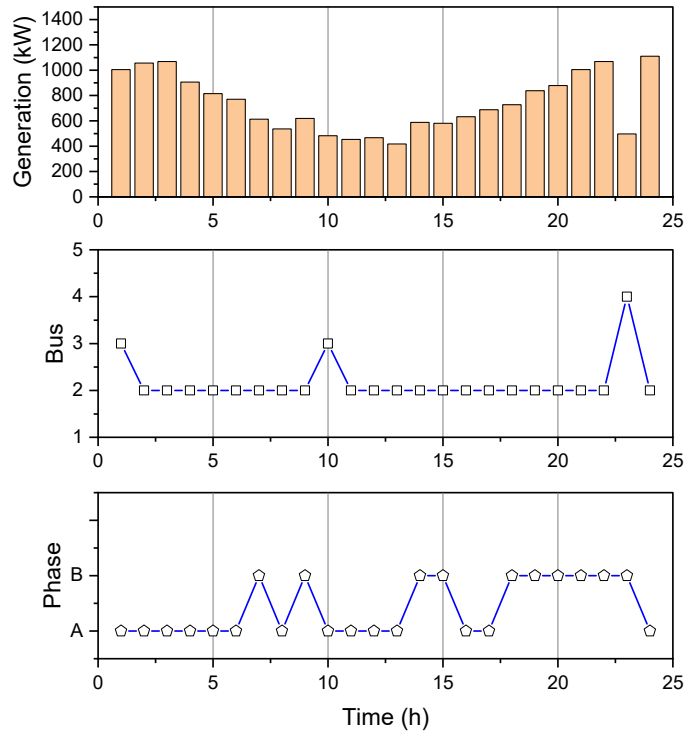


Figure 7. Optimal results of the WT's power generation, bus, and phase locations.

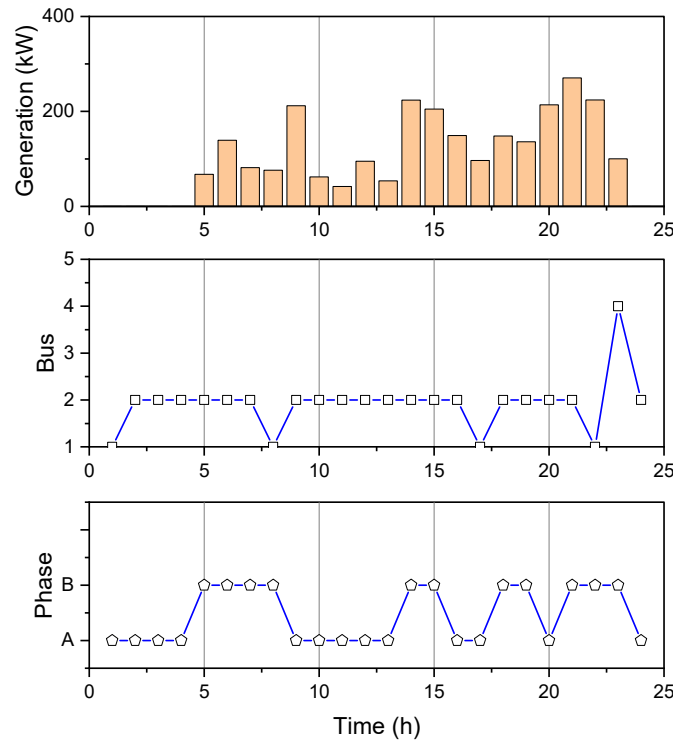


Figure 8. Optimal results of the DG's power generation, bus, and phase locations.

It can be observed from Figure 9 that the MT outputs are maximized at Bus 2, and Phase B in particular has been found to be very effective during peak hours. The fact that MT generation coincides with demand peaks points to its potential contribution to enhancing the resilience of the system. Future plans of expansion should be biased toward areas with higher MT outputs so as to maintain a balanced energy supply.

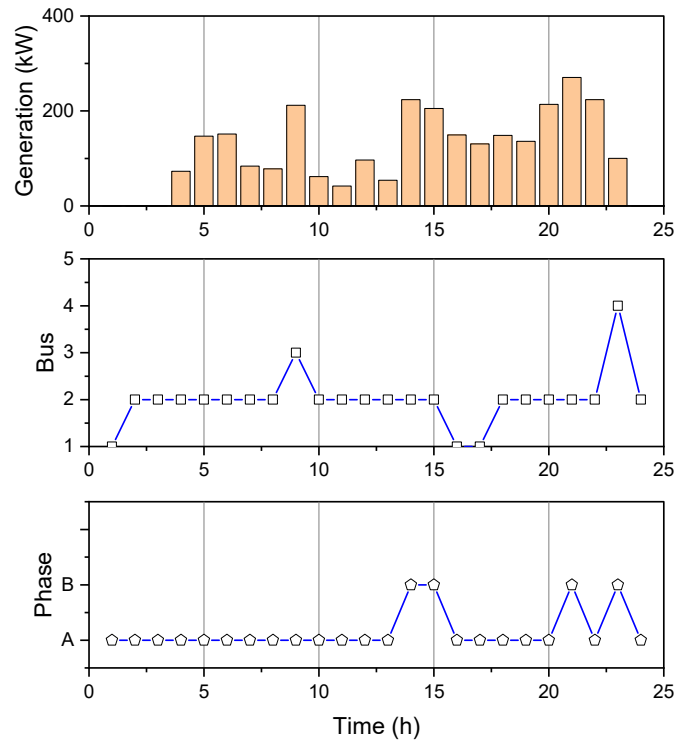


Figure 9. Optimal results of the MT's power generation, bus, and phase locations.

The BESS is, according to Figure 10, most effective at Bus 2. It is capable of providing power during evening peak loads and replenishes its capacity by charging during the day. Placement of the ESS in this location serves to enable superior management of the energy flows to ensure that any excess generation from the PV and WT is valorized effectively.

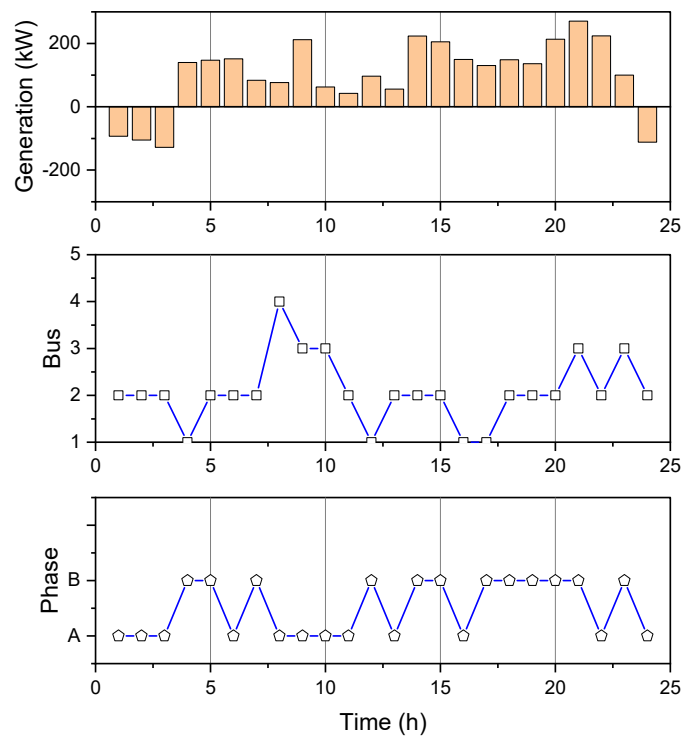


Figure 10. Optimal results of the BESS's power generation, bus, and phase locations.

On the whole, the results depict Bus 2 as the best place of location for most of the generation options, especially in Phase A. This means that there is a need to have a proper site assessment during the actual planning of renewable energy projects and also at the deployment of the DGs. The final result of the outcome is used in showing how critical location and phase selection are in enhancing the efficiency and reliability of the energy system and therefore in ensuring a more robust and sustainable power network.

5.5. Impact of the Proposed Model on Voltage Deviation, Energy Losses, and Costs

The proposed model has huge consequences for, but not limited to, key performance indicators like voltage deviation, energy losses, and operational costs. A deeper look into such impacts is presented which proves the effectiveness of the model in enhancing the overall stability, efficiency, and, therefore, economic viability of the network.

The significant voltage stability improvements were realized after the execution of the proposed model within the studied periods. Figure 11 clearly shows that the values of VD (voltage deviation) were always about 1.489 to 1.490, representing a significant deviation with significant questions about the reliability of the distribution network. After implementation, the VD was proven to reduce significantly during peak operational hours. For example, in the first hour, the VD reduced from 1.48966502 p.u to 1.340699 p.u, and similar patterns continued throughout the entire day, as depicted with the 24th hour reducing from 1.48970899 p.u to 1.340902 p.u. The foregoing results totally represent how well the model works in controlling voltage deviations, thus enhancing power delivery stability and reliability within microgrids.

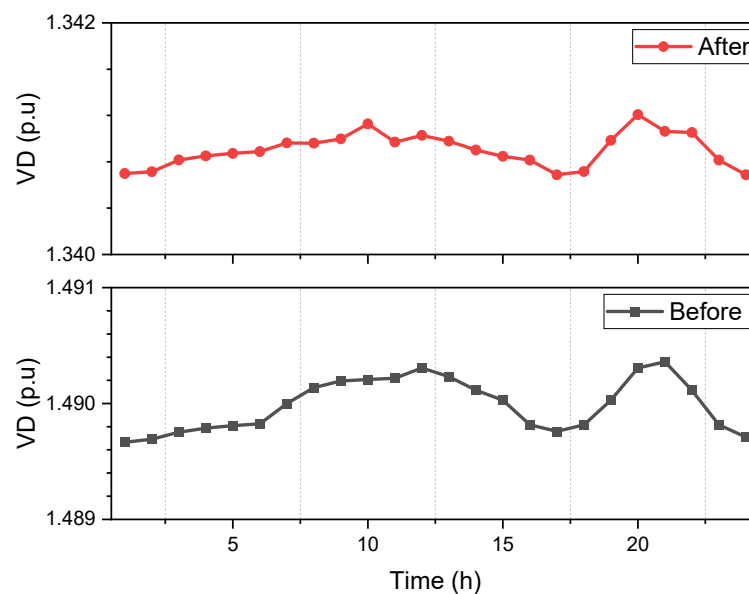


Figure 11. Voltage deviations before and after the proposed optimization EM model.

Among other elements, the model has provided voltage stability. There was also a significant reduction in the loss of energy. Figure 12 shows the reduction in energy loss to be constant both before and after the implementation of the model. Before optimization, the losses were at their peak of 37.10 kW during hour 21. However, with the use of the proposed model, energy losses went down considerably: in hour 1, energy losses went from 9.61 kW to 8.66 kW, while, by hour 24, the extra losses were from 11.44 kW to 9.95 kW, reflecting improved system efficiency. Total energy losses, which were 499.76 kW before implementation, went down to 446.65 kW after implementation, underlining the capability of the model for optimization in energy distribution and indicating that less energy loss occurs.

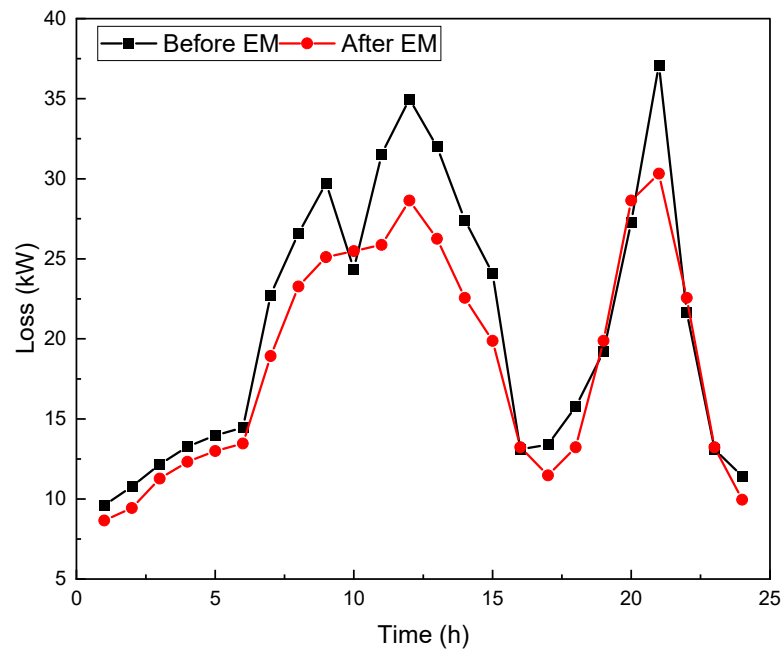


Figure 12. Microgrid losses before and after the proposed optimization EM model.

In the end, the model contributed to a significant impact on the total costs related to different sources in the microgrid generations.

The total microgrid operation cost with RESs is USD 220,921.39, as represented in Table 3. Compared to a non-RES scenario, which was a total of USD 1,324,587, this is a huge cost reduction. In detail, the breakdown includes the following: PV at USD 8667.05, grid power at USD 20,756.11, WTs at USD 40,142.04, and distributed generation at USD 38,145.56. Added to this are microturbines at USD 8715.11 and ESS at USD 61,655.70, while DR accounted for USD 42,839.82.

Table 3. Daily costs of the test system using proposed method.

	PV	Grid	WT	DG	MT	BESS	DR	Total
Cost (USD)	8667.055	20,756.11	40,142.04	38,145.56	8715.105	61,655.7	42,839.82	220,921.3863

The huge cost difference underlines the financial advantages of integrating RES into the microgrid, thus proving it feasible both from an environmental and economic point of view. These findings should be able to validate the proposed model with voltage stability improvement, energy loss reductions, and huge cost savings. Thus, a robust solution for the optimization of MGs can be derived.

5.6. Results Comparison with Other Algorithms and Stochastic Methods

This section compares the performance of the proposed ECOA with other techniques that traditionally have been used in microgrid management. For this purpose, the main performance indicator under study is the fitness function values J_{total}^{UT} .

In optimization algorithms, various parameters play a crucial role in determining their performance and effectiveness. For instance, in the HPSO-GSA, the parameters are set as follows: $w_{max} = 0.9$ and $w_{min} = 0.4$ (inertia weights), and $c_{1min} = 0.5$, $c_{1max} = 2.5$, $c_{2min} = 0.5$, and $c_{2max} = 2.5$ (cognitive and social coefficients) [9]. The parameter $Tf = 20$ represents the iteration interval cycle and $S_{min} = 4$ refers to the minimum size of the swarm. Similarly, the GPSOA employs parameters such as $c_3 = c_4 = 0.5$ (acceleration factors) along with $\omega_{max} = 0.9$, $\omega_{min} = 0.4$, and $c_1 = c_2 = 2$ (cognitive and social factors) [8]. The PSO algorithm typically uses $\omega = 0.7$ (inertia weight) with $c_1 = c_2 = 2$ (cognitive and social coefficients). The GA is characterized by a crossover rate of 0.8 and a mutation rate of 0.1. In

contrast, our proposed ECOA does not require parameter settings, similar to the traditional CO algorithm [45], which streamlines its implementation and enhances its applicability in diverse optimization scenarios.

The simulation results show that the ECOA outperforms the applied traditional and hybrid optimization techniques. As reflected in Table 4, the best minimum fitness value gained by the ECOA was 2.090865, with its maximum value being 2.101378, featuring a mean of 2.089554 and a small standard deviation of 0.01126, representing the high stability and reliability of the ECOA. For its part, the GA has an average fitness of 2.412126; PSO and the conventional CO algorithm reached means of 2.33533 and 2.225719, respectively.

Table 4. Comparative results of the fitness function values ($J_{\text{total}}^{\text{UT}}$) obtained by the applied Optimization Algorithms.

Algorithm	Min	Max	Mean	SD	CPU Time (s)
GA	2.346278	2.46748	2.412126	0.031894	67.65
PSO	2.283724	2.393773	2.33533	0.02973	42.15
CO	2.187906	2.286634	2.225719	0.02943	55.02
GPSOA	2.120345	2.210457	2.145893	0.025870	51.47
HPSO-GSA	2.105437	2.202345	2.135672	0.020110	57.85
ECOA	2.090865	2.101378	2.089554	0.01126	46.26

Furthermore, the GPSOA and HPSO-GSA hybrid algorithms also demonstrated competitive performance, with mean fitness values of 2.145893 and 2.135672, respectively. These results underline the effectiveness of hybrid algorithms in enhancing optimization outcomes in microgrid management. In addition, as can be seen from Table 4, the ECOA's CPU time of 46.26 s indicates that this algorithm has good competitiveness in terms of effectively throwing a balance between its efficiency and performance. In contrast, the GA took 67.65 s, meaning that, besides producing worse optimal results, it was even slower compared to the ECOA.

Moreover, the GPSOA and HPSO-GSA also exhibited competitive results, with minimum fitness values of 2.120345 and 2.105437, respectively, and CPU times of 51.47 s and 57.85 s. Although both hybrid algorithms showed improved performance over the GA, the ECOA remains the superior choice regarding both optimal results and computational efficiency.

Looking closer, the convergence characteristic is somewhat different, as shown in Figure 13. The highest value of 3.5 was initiated by the GA, which showed relatively slow convergence with noticeable fluctuations during the first iterations that then stabilized after the thirty-fifth iteration, with a value of around 2.346278. Thus, the final value was approached rather gently, and the convergence behavior followed a step-like pattern. Meanwhile, PSO started from a relatively lower point, 3.0, and decreased much more smoothly before converging to 2.283724 until iteration 60. This one turned out to be an immensely smoother algorithm where the fitness curve did not suddenly increase erroneously often, which indicates the strength of this algorithm in spreading its coverage over the solution space. Meanwhile, the behavior of the conventional CO algorithm was similar, starting at approximately 3.1, and, after 40 iterations, it converged to 2.187906. Yet, its convergence was marked by slower fitness reductions compared to the ECOA, and hence it was less efficient in its approach to the optimal solution.

While all other algorithms were showing convergence attitudes, the ECOA, however, showed the fastest convergence rate among the compared algorithms. This algorithm, with an initial value starting at around 3.0, has successfully fallen below its fitness to 2.090865 within just 30 iterations and has kept that value constant, with a maximum of limited fluctuation thereafter. Thus, the ECOA's convergence curve is comparatively smooth, indicating that this algorithm executes accordingly in minimizing an objective function in uncertain renewable generation conditions.

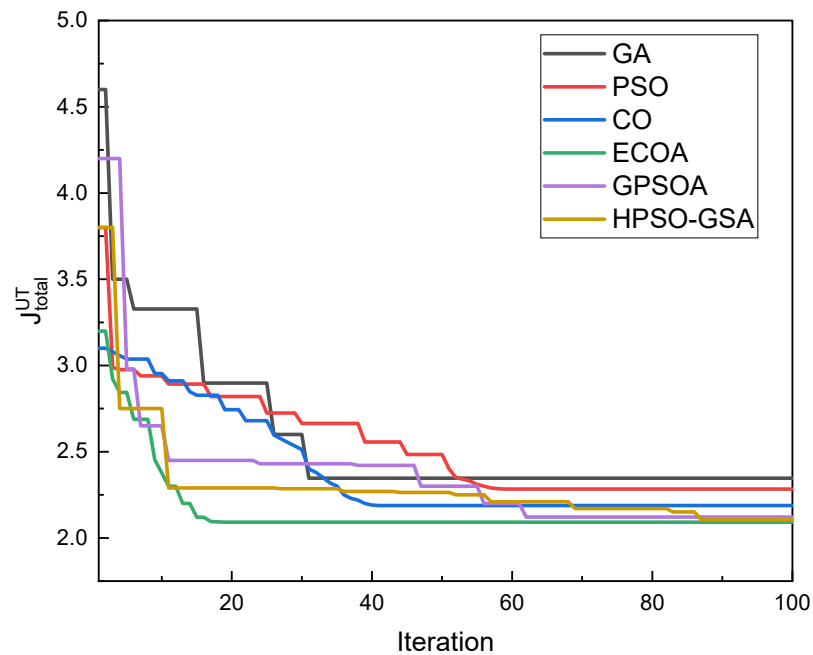


Figure 13. Convergence curves of the comparative algorithms in solving the problem.

The hybrid algorithms, GPSOA and HPSO-GSA, also exhibit competitive convergence characteristics. However, the ECOA’s overall speed and stability remain advantageous: the GPSOA starts from a higher initial value of 4.2 and shows a gradual reduction, reaching a fitness of around 2.12035 by iteration 70. Additionally, while the GPSOA maintains a smooth convergence curve, its rate of descent is slower than the ECOA’s. This indicates that the GPSOA, though efficient, is less aggressive in its convergence approach compared to the ECOA’s rapid optimization. The HPSO-GSA, which begins at an initial value of 3.8, demonstrates a slightly faster convergence than the GPSOA, reaching a final fitness of 2.10544 by iteration 60. The HPSO-GSA’s stable curve and minimal fluctuations indicate an effective performance; however, the ECOA still outpaces it, reaching an optimal value in fewer iterations.

These findings show that the ECOA is indeed a powerful and effective technique for the management of microgrid systems, especially when their operation is under uncertain renewable generations.

Finally, to better understand the performance of the proposed UT approach, simulation results are further analyzed together with other stochastic frameworks such as MCS and the PEM. In Table 5, the proposed UT has a cost function value of $J_{total}^{UT} = 2.090865$, which is competitive in accuracy against the MCS at a higher value of 2.091234.

Table 5. Comparison of Cost Function Value in Different Stochastic Frameworks.

Method	J_{total}^{UT}	CPU Time (s)
MCS [10]	2.091234	137.00
PEM [18]	2.090950	37.10
Proposed UT	2.090865	46.26

While the MCS indeed gave a comprehensive representation of the uncertainties, it required significantly more computational time (137 s) compared with both the PEM at 37.10 s and the proposed UT method at 46.26 s. The results show that the UT approach does strike a good balance in terms of performance for both computational efficiency and accuracy, hence being robust in performing microgrid management under uncertainty.

5.7. Discussion

The results from this work identified the ECOA in terms of optimizing microgrid management. The results clearly depict the ECOA as outperforming all traditional and hybrid optimization techniques, such as the GA, PSO, the conventional CO, the GPSOA, and the HPAO-GSA, by most of the key performance indicators. The statistical analysis of the fitness function provides supportive evidence for the ECOA in terms of performance, where the average value is 2.090865 with a low standard deviation of 0.01126. Therefore, it proves that the algorithm is capable of dealing with various operating conditions in a consistent and reliable mandate, which plays an important role in microgrid applications due to the high variability and uncertainty associated with the integration of renewable sources.

Table 6 presents a comparison of optimization algorithms applied to microgrid management, focusing on key performance attributes such as convergence speed, final fitness value, stability, computational efficiency, and exploration–exploitation balance. The ECOA stands out with the fastest convergence rate, the lowest final fitness value, and a consistently smooth stability profile, indicating its effectiveness in achieving optimal solutions under uncertain conditions. The GPSOA and HPSO-GSA exhibit a balanced exploration–exploitation approach and moderate stability, though they converge at a slower rate than the ECOA. This comparison highlights the ECOA’s robust performance in minimizing objective functions, which is especially suited for renewable energy scenarios that require rapid, stable convergence.

Table 6. Comparison of optimization algorithms based on key performance attributes.

Algorithm	Convergence Speed	Final Fitness Value	Stability	Computational Efficiency	Exploration–Exploitation Balance
GA	Moderate	Moderate	Moderate	Moderate	Low
PSO	Moderate	High	High	Moderate	Moderate
CO	Moderate	Moderate	Moderate	High	Low
ECOA	High	Very Low	Very High	High	Balanced
GPSOA	Moderate	Low	Moderate	Moderate	Balanced
HPSO-GSA	Moderate	Low	High	Moderate	Balanced

The reduction in voltage deviation, as realized across the run, demonstrates how effective the proposed model is in enhancing voltage stability across the microgrid. The VD values in the network before optimization were relatively high and consistent, which could tend to pose potential instability and reliability concerns in practical scenarios. With the application of the ECOA in conjunction with UT, it can be observed that the model minimized these VD values substantially by up to 10%. These improved voltage profiles in all time periods indeed confirm the relevance of using advanced optimization techniques in order to provide flat voltage profiles, especially in unbalanced distribution networks with high RES penetration. This will be very important when trying to handle intermittent systems like PV systems and WTs, which may create disturbances in generation and further deteriorate voltage imbalances.

The model applied in this contribution has reduced energy losses significantly. Before optimization, high energy losses were witnessed, especially during peak demand periods. In this context, the presented model performs an efficient dispatch of resources of generation, including PV systems, WTs, DG, MTs, and the BESS, which enhances overall efficiencies within the microgrid system. This is the capability of the model in streamlining the process of energy distribution to cut down on wastages to improve efficiency. The reduction from 499.77 kW to 446.65 kW is proof of the reduction in losses, which is very important in the sense that reduced losses translate into more efficient energy usage, reduced environmental impacts, and lower operating costs for microgrid operators in the long term.

Perhaps the most striking result is the drastic reduction in total operational costs when renewable energy sources were integrated into the microgrid. This put the total cost of operation with RES integration at USD 220,921.39 against USD 1,324,587 without RES. The large difference in cost indicates the economic viability of integrating renewable energy into microgrids. Furthermore, the breakdown of the costs shows a relative decrease in overall operational costs with the inclusion of RESs like PV systems and WTs. Additionally, the BESS and DR programs will serve to optimize energy consumption patterns and further reduce dependence on these relatively highly valued external sources of energy. Results also show that further investment in RESs and storage technologies could lead to larger long-term cost savings, hence supporting the transition toward more sustainable and cost-effective energy management frameworks.

A number of limitations exist in the present model. The price modeling for the optimization process is simplified and does not fully capture the complexities inherent in real-world electricity pricing structures, which are influenced by market fluctuations, time-of-use (TOU) rates, and demand elasticity. This simplification may reduce the model's ability to accurately reflect the economic signals that drive consumer behavior and energy consumption patterns.

While the model has demonstrated significant improvements across various performance metrics, concerns regarding the computational efficiency of the Enhanced Cheetah Optimization Algorithm (ECO) persist, particularly when applied to larger-scale microgrid systems. The algorithm's performance may vary under different environmental and demand conditions, especially when confronted with extreme fluctuations in renewable energy outputs or sudden changes in load patterns. This variability could affect both the convergence speed of the algorithm and the quality of the optimal solution.

Furthermore, the issues of improving computational efficiency and scalability will be paramount in ensuring the practical applications of the model. Future research could explore adaptive mechanisms within the ECO to enhance its responsiveness to changing conditions as well as strategies for managing scalability. Hierarchical optimization approaches and parallel processing capabilities could extend the applicability of the proposed method across diverse microgrid scenarios.

In general, the ECO has proven to be a robust optimization tool for microgrid management, effectively addressing the challenges posed by renewable energy integration and load variability. The notable improvements in voltage stability, energy efficiency, and cost reduction exhibited by the proposed model contribute to the development of more resilient and sustainable power systems. Addressing the identified limitations will be crucial for enhancing the model's performance and applicability in real-world scenarios. Overall, the results offer a promising pathway for sustainable energy management practices and the integration of higher levels of renewable energy into the grid, underscoring the need for continuous research and innovation in this field.

6. Conclusions

This paper presents a comprehensive framework for optimizing microgrid management by integrating the Enhanced Cheetah Optimization Algorithm (ECO) with Unscented Transformation (UT). The proposed model effectively addresses the complexities associated with variable renewable energy sources and fluctuating load demands, resulting in significant improvements in key performance metrics. Specifically, the optimization yielded an overall cost of operation of USD 220,921.39, representing a reduction of over 83% reduction, a decrease in overall power losses to 446.65 W (more than 10%), and an excellent voltage stability deviation of 10%. The integration of UT enhances decision-making under uncertainty, allowing for the precise propagation of variability through nonlinear functions, which is critical for effective energy management in environments with fluctuating renewable generation. While the proposed optimization framework demonstrates significant effectiveness, the performance of the Enhanced Cheetah Optimization Algorithm (ECO) may fluctuate under varying environmental and demand conditions, especially

during extreme shifts in renewable energy output or sudden changes in load patterns. Such variability can influence the algorithm's convergence speed and the quality of the optimal solution. Future research could investigate the development of adaptive mechanisms within the ECOA to improve its responsiveness to these changing conditions. Additionally, although the current framework shows effectiveness in terms of the specified microgrid configurations, its scalability to larger systems or more complex microgrid architectures requires further exploration. Strategies for managing scalability—such as hierarchical optimization approaches or parallel processing capabilities—could be developed to broaden the applicability of the proposed method across diverse microgrid scenarios. To enhance the model's performance in dynamic energy environments, future research should also consider integrating adaptive forecasting techniques and investigating emerging technologies.

Funding: This research was funded by Deanship of Postgraduate Studies and Scientific Research at Majmaah University, project number: ER-2024-1406.

Data Availability Statement: The data presented in this study are available in this article.

Acknowledgments: The author extends the appreciation to the Deanship of Postgraduate Studies and Scientific Research at Majmaah University for funding this research work through the project number (ER-2024-1406).

Conflicts of Interest: The authors declare no conflicts of interest.

References

- Zia, M.F.; Elbouchikhi, E.; Benbouzid, M. Microgrids Energy Management Systems: A Critical Review on Methods, Solutions, and Prospects. *Appl. Energy* **2018**, *222*, 1033–1055. [\[CrossRef\]](#)
- Kumari, B.A.; Vaisakh, K. Integration of Solar and Flexible Resources into Expected Security Cost with Dynamic Optimal Power Flow Problem Using a Novel DE Algorithm. *Renew. Energy Focus* **2022**, *42*, 48–69. [\[CrossRef\]](#)
- Fathi, R.; Tousi, B.; Galvani, S. A New Approach for Optimal Allocation of Photovoltaic and Wind Clean Energy Resources in Distribution Networks with Reconfiguration Considering Uncertainty Based on Info-Gap Decision Theory with Risk Aversion Strategy. *J. Clean. Prod.* **2021**, *295*, 125984. [\[CrossRef\]](#)
- Ghadikolaie, E.R.; Ghafouri, A.; Sedighi, M. Probabilistic Energy Management of DGs and Electric Vehicle Parking Lots in a Smart Grid Considering Demand Response. *Int. J. Energy Res.* **2024**, *2024*, 5543500. [\[CrossRef\]](#)
- Almadhor, A.; Rauf, H.T.; Khan, M.A.; Kadry, S.; Nam, Y. A Hybrid Algorithm (BAPSO) for Capacity Configuration Optimization in a Distributed Solar PV Based Microgrid. *Energy Rep.* **2021**, *7*, 7906–7912. [\[CrossRef\]](#)
- Elymany, M.M.; Enany, M.A.; Elsonbaty, N.A. Hybrid Optimized-ANFIS Based MPPT for Hybrid Microgrid Using Zebra Optimization Algorithm and Artificial Gorilla Troops Optimizer. *Energy Convers. Manag.* **2024**, *299*, 117809. [\[CrossRef\]](#)
- Kumar, S.S.; Iruthayarajan, M.W.; Saravanan, R. Hybrid Technique for Optimizing Charging-Discharging Behaviour of EVs and Demand Response for Cost-Effective PV Microgrid System. *J. Energy Storage* **2024**, *96*, 112667. [\[CrossRef\]](#)
- Jiang, S.; Zhang, C.; Wu, W.; Chen, S. Combined Economic and Emission Dispatch Problem of Wind-thermal Power System Using Gravitational Particle Swarm Optimization Algorithm. *Math. Probl. Eng.* **2019**, *2019*, 5679361. [\[CrossRef\]](#)
- Jiang, S.; Zhang, C.; Chen, S. Sequential Hybrid Particle Swarm Optimization and Gravitational Search Algorithm with Dependent Random Coefficients. *Math. Probl. Eng.* **2020**, *2020*, 1957812. [\[CrossRef\]](#)
- Hashish, M.S.; Hasaniien, H.M.; Ji, H.; Alkuhayli, A.; Alharbi, M.; Akmaral, T.; Turkey, R.A.; Jurado, F.; Badr, A.O. Monte Carlo Simulation and a Clustering Technique for Solving the Probabilistic Optimal Power Flow Problem for Hybrid Renewable Energy Systems. *Sustainability* **2023**, *15*, 783. [\[CrossRef\]](#)
- Saha, A.; Bhattacharya, A.; Das, P.; Chakraborty, A.K. A Novel Approach towards Uncertainty Modeling in Multiobjective Optimal Power Flow with Renewable Integration. *Int. Trans. Electr. Energy Syst.* **2019**, *29*, e12136. [\[CrossRef\]](#)
- Ullah, Z.; Qazi, H.S.; Alferidi, A.; Alsolami, M.; Lami, B.; Hasaniien, H.M. Optimal Energy Trading in Cooperative Microgrids Considering Hybrid Renewable Energy Systems. *Alex. Eng. J.* **2024**, *86*, 23–33. [\[CrossRef\]](#)
- Ahn, H.; Rim, D.; Pavlak, G.S.; Freihaut, J.D. Uncertainty Analysis of Energy and Economic Performances of Hybrid Solar Photovoltaic and Combined Cooling, Heating, and Power (CCHP + PV) Systems Using a Monte-Carlo Method. *Appl. Energy* **2019**, *255*, 113753. [\[CrossRef\]](#)
- Shahbazi, A.; Moradi CheshmehBeigi, H.; Abdi, H.; Shahbazitabar, M. Probabilistic Optimal Allocation of Electric Vehicle Charging Stations Considering the Uncertain Loads by Using the Monte Carlo Simulation Method. *J. Oper. Autom. Power Eng.* **2023**, *11*, 277–284.
- Ahmed, D.; Ebeed, M.; Kamel, S.; Nasrat, L.; Ali, A.; Shaaban, M.F.; Hussien, A.G. An Enhanced Jellyfish Search Optimizer for Stochastic Energy Management of Multi-Microgrids with Wind Turbines, Biomass and PV Generation Systems Considering Uncertainty. *Sci. Rep.* **2024**, *14*, 15558. [\[CrossRef\]](#) [\[PubMed\]](#)

16. Alavi, S.A.; Ahmadian, A.; Aliakbar-Golkar, M. Optimal Probabilistic Energy Management in a Typical Micro-Grid Based-on Robust Optimization and Point Estimate Method. *Energy Convers. Manag.* **2015**, *95*, 314–325. [[CrossRef](#)]
17. Xiao, F.; Ai, Q. New Modeling Framework Considering Economy, Uncertainty, and Security for Estimating the Dynamic Interchange Capability of Multi-Microgrids. *Electr. Power Syst. Res.* **2017**, *152*, 237–248. [[CrossRef](#)]
18. Habibi, S.; Effatnejad, R.; Hedayati, M.; Hajihosseini, P. Stochastic Energy Management of a Microgrid Incorporating Two-Point Estimation Method, Mobile Storage, and Fuzzy Multi-Objective Enhanced Grey Wolf Optimizer. *Sci. Rep.* **2024**, *14*, 1667. [[CrossRef](#)]
19. Aien, M.; Fotuhi-Firuzabad, M.; Aminifar, F. Probabilistic Load Flow in Correlated Uncertain Environment Using Unscented Transformation. *IEEE Trans. Power Syst.* **2012**, *27*, 2233–2241. [[CrossRef](#)]
20. Lin, X.; Shu, T.; Tang, J.; Yang, Y.; Liu, F.; Zheng, J.; Peng, S. An Unscented Transformation Based Probabilistic Power Flow for Autonomous Hybrid AC/DC Microgrid with Correlated Uncertainty Sources. In Proceedings of the 2018 2nd IEEE Conference on Energy Internet and Energy System Integration (EI2), Beijing, China, 20–22 October 2018; pp. 1–6.
21. Kavousi-Fard, A.; Niknam, T.; Akbari-Zadeh, M.-R.; Dehghan, B. Stochastic Framework for Reliability Enhancement Using Optimal Feeder Reconfiguration. *J. Syst. Eng. Electron.* **2014**, *25*, 901–910. [[CrossRef](#)]
22. Oke, O.; Ozgonenel, O.; Thomas, D.W.P.; Ataseven, M.S. Probabilistic Load Flow of Unbalanced Distribution Systems with Wind Farm. *Teh. Vjesn.* **2019**, *26*, 1260–1266.
23. Kurt, U.; Ozgonenel, O.; Ayvaz, B.B. Probabilistic Power Flow Analysis Using Matlab Graphical User Interface (GUI). *J. Electr. Eng. Technol.* **2022**, *17*, 929–943. [[CrossRef](#)]
24. Zhang, Y.; Gatsis, N.; Giannakis, G.B. Robust Energy Management for Microgrids With High-Penetration Renewables. *IEEE Trans. Sustain. Energy* **2013**, *4*, 944–953. [[CrossRef](#)]
25. Carli, R.; Cavone, G.; Pippia, T.; Schutter, B.D.; Dotoli, M. Robust Optimal Control for Demand Side Management of Multi-Carrier Microgrids. *IEEE Trans. Autom. Sci. Eng.* **2022**, *19*, 1338–1351. [[CrossRef](#)]
26. Balderrama, S.; Lombardi, F.; Riva, F.; Canedo, W.; Colombo, E.; Quoilin, S. A Two-Stage Linear Programming Optimization Framework for Isolated Hybrid Microgrids in a Rural Context: The Case Study of the “El Espino” Community. *Energy* **2019**, *188*, 116073. [[CrossRef](#)]
27. Yoon, C.; Park, Y.; Sim, M.K.; Lee, Y.I. A Quadratic Programming-Based Power Dispatch Method for a DC-Microgrid. *IEEE Access* **2020**, *8*, 211924–211936. [[CrossRef](#)]
28. Nemati, M.; Braun, M.; Tenbohlen, S. Optimization of Unit Commitment and Economic Dispatch in Microgrids Based on Genetic Algorithm and Mixed Integer Linear Programming. *Appl. Energy* **2018**, *210*, 944–963. [[CrossRef](#)]
29. Ruder, S. An Overview of Gradient Descent Optimization Algorithms. *arXiv* **2016**, arXiv:1609.04747.
30. Dennis John, E.J.; Moré, J.J. Quasi-Newton Methods, Motivation and Theory. *SIAM Rev.* **1977**, *19*, 46–89. [[CrossRef](#)]
31. Riley, J.; Butler, R.; Ogilvie, D.; Finniear, R.; Jenner, D.; Powell, S.; Anand, R.; Smith, J.C.; Markham, A.F. A Novel, Rapid Method for the Isolation of Terminal Sequences from Yeast Artificial Chromosome (YAC) Clones. *Nucleic Acids Res.* **1990**, *18*, 2887–2890. [[CrossRef](#)]
32. Goldberg, D.E. *Genetic Algorithms*; Pearson Education India: Bangalore, India, 2013; ISBN 817758829X.
33. Kennedy, J.; Eberhart, R. Particle Swarm Optimization. In Proceedings of the ICNN’95-International Conference on Neural Networks, Perth, WA, Australia, 27 November–1 December 1995; Volume 4, pp. 1942–1948.
34. Karimi, H.; Jadid, S. Optimal Energy Management for Multi-Microgrid Considering Demand Response Programs: A Stochastic Multi-Objective Framework. *Energy* **2020**, *195*, 116992. [[CrossRef](#)]
35. Li, Z.; Zang, C.; Zeng, P.; Yu, H.; Li, H. Two-Stage Stochastic Programming Based Model Predictive Control Strategy for Microgrid Energy Management under Uncertainties. In Proceedings of the 2016 International Conference on Probabilistic Methods Applied to Power Systems (PMAPS), Beijing, China, 16–20 October 2016; pp. 1–6.
36. Yu, D.; Zhu, H.; Han, W.; Holburn, D. Dynamic Multi Agent-Based Management and Load Frequency Control of PV/Fuel Cell/Wind Turbine/CHP in Autonomous Microgrid System. *Energy* **2019**, *173*, 554–568. [[CrossRef](#)]
37. Anand, H.; Ramasubbu, R. A Real Time Pricing Strategy for Remote Micro-Grid with Economic Emission Dispatch and Stochastic Renewable Energy Sources. *Renew. Energy* **2018**, *127*, 779–789. [[CrossRef](#)]
38. Gholami, K.; Dehnavi, E. A Modified Particle Swarm Optimization Algorithm for Scheduling Renewable Generation in a Micro-Grid under Load Uncertainty. *Appl. Soft Comput.* **2019**, *78*, 496–514. [[CrossRef](#)]
39. Kreishan, M.Z.; Zobaa, A.F. Mixed-Integer Distributed Ant Colony Optimization of Dump Load Allocation with Improved Islanded Microgrid Load Flow. *Energies* **2023**, *16*, 4257. [[CrossRef](#)]
40. Jumani, T.A.; Mustafa, M.W.; Rasid, M.M.; Memon, Z.A. Dynamic Response Enhancement of Grid-Tied Ac Microgrid Using Salp Swarm Optimization Algorithm. *Int. Trans. Electr. Energy Syst.* **2020**, *30*, e12321. [[CrossRef](#)]
41. Sen, S.; Gupta, K.D.; Poudyal, S.; Ahsan, M.M. A Genetic Algorithm Approach to Optimize Dispatching for a Microgrid Energy System with Renewable Energy Sources. In Proceedings of the CS & IT Conference Proceedings, Dubai, United Arab Emirates, 23–24 February 2019; Volume 9.
42. Qazi, S.H.; Mustafa, M.W.; Sultana, U.; Mirjat, N.H.; Soomro, S.A.; Rasheed, N. Regulation of Voltage and Frequency in Solid Oxide Fuel Cell-Based Autonomous Microgrids Using the Whales Optimisation Algorithm. *Energies* **2018**, *11*, 1318. [[CrossRef](#)]
43. Tayab, U.B.; Lu, J.; Taghizadeh, S.; Metwally, A.S.M.; Kashif, M. Microgrid Energy Management System for Residential Microgrid Using an Ensemble Forecasting Strategy and Grey Wolf Optimization. *Energies* **2021**, *14*, 8489. [[CrossRef](#)]

44. Bukar, A.L.; Tan, C.W.; Lau, K.Y. Optimal Sizing of an Autonomous Photovoltaic/Wind/Battery/Diesel Generator Microgrid Using Grasshopper Optimization Algorithm. *Sol. Energy* **2019**, *188*, 685–696. [[CrossRef](#)]
45. Akbari, M.A.; Zare, M.; Azizipanah-Abarghooee, R.; Mirjalili, S.; Deriche, M. The Cheetah Optimizer: A Nature-Inspired Metaheuristic Algorithm for Large-Scale Optimization Problems. *Sci. Rep.* **2022**, *12*, 1–20. [[CrossRef](#)]
46. Nowdeh, S.A.; Naderipour, A.; Davoudkhani, I.F.; Guerrero, J.M. Stochastic Optimization-Based Economic Design for a Hybrid Sustainable System of Wind Turbine, Combined Heat, and Power Generation, and Electric and Thermal Storages Considering Uncertainty: A Case Study of Espoo, Finland. *Renew. Sustain. Energy Rev.* **2023**, *183*, 113440. [[CrossRef](#)]
47. Kersting, W.H. Radial Distribution Test Feeders. In Proceedings of the 2001 IEEE Power Engineering Society Winter Meeting. Conference Proceedings (Cat. No.01CH37194), Columbus, OH, USA, 28 January–1 February 2001; Volume 2, pp. 908–912.
48. Alilou, M.; Nazarpour, D.; Shayeghi, H. Multi-Objective Optimization of Demand Side Management and Multi Dg in the Distribution System with Demand Response. *J. Oper. Autom. Power Eng.* **2018**, *6*, 230–242.
49. Sedighzadeh, M.; Fazlhashemi, S.S.; Javadi, H.; Taghvaei, M. Multi-Objective Day-Ahead Energy Management of a Microgrid Considering Responsive Loads and Uncertainty of the Electric Vehicles. *J. Clean. Prod.* **2020**, *267*, 121562. [[CrossRef](#)]
50. Abou El-Ela, A.A.; El-Sehiemy, R.A.; Kinawy, A.-M.; Ali, E.S. Optimal Placement and Sizing of Distributed Generation Units Using Different Cat Swarm Optimization Algorithms. In Proceedings of the 2016 Eighteenth International Middle East Power Systems Conference (MEPCON), Cairo, Egypt, 27–29 December 2016; pp. 975–981.

Disclaimer/Publisher’s Note: The statements, opinions and data contained in all publications are solely those of the individual author(s) and contributor(s) and not of MDPI and/or the editor(s). MDPI and/or the editor(s) disclaim responsibility for any injury to people or property resulting from any ideas, methods, instructions or products referred to in the content.